Linköping University Medical Dissertations No. 1109

# Noninvasive Evaluation of Myocardial Ischemia and Left Ventricular Function

**Eva Maret**

Division of Cardiovascular Medicine
Department of Medical and Health Sciences
Linköping University, Sweden


Linköping University
FACULTY OF HEALTH SCIENCES

**Linköping 2009**

Cover picture/illustration: William Björklund



Printed in Sweden by LiU-Tryck, Linköping, Sweden, 2009

ISBN 978-91-7393-675-0
ISSN 0345-0082

*To Martin and John!*

Somewhere over the rainbow
Way up high,
There's a land that I heard of
Once in a lullaby.

Somewhere over the rainbow
Skies are blue,
And the dreams that you dare to dream
Really do come true.

From “The Wizard of OZ”, music by Harold Arlen
and lyrics by E.Y. Harburg

# CONTENTS

# SUMMARY

The general aim of this thesis was, following the path of the ischemic cascade, to evaluate the feasibility of some new non-invasive techniques for the detection of myocardial ischemia, the extent of infarcted myocardium, and for the quantification of systolic left ventricular function.

Reduced longitudinal myocardial velocity and displacement may be early signs of ischemia. We evaluated the diagnostic sensitivity and specificity of pulsed tissue Doppler for the detection of ischemia and scar during dobutamine stress testing and compared it with myocardial perfusion scintigraphy (SPECT) in patients with a history of unstable angina. Pulsed tissue Doppler was useful for objective quantification of left ventricular longitudinal shortening and for differentiation between patients with a normal, ischemic or necrotic myocardium.

The coronary flow velocity reserve (CFVR) of the left anterior descending artery (LAD) was studied with transthoracic Doppler echocardiography (TTDE) during adenosine stress. Patients with a clinical suspicion of stress induced myocardial ischemia were investigated, and the results were compared with the findings from SPECT. A CFVR >2 in the LAD could exclude significant coronary artery disease in a clinical setting, however, in cases with low CFVR, multiple cardiovascular and metabolic risk factors as well as epicardial coronary artery disease or microvascular dysfunction might be responsible. TTDE is a promising tool, e.g. for follow-up after coronary interventions or for evaluating endothelial function over time.

A third study focused on the importance of accurate and reproducible measurements of left ventricular volumes and ejection fraction (LVEF). Patients with known or suspected coronary artery disease with different levels of LVEF were enrolled. We compared the LVEF determined with an automatic echocardiographic method with manual planimetry, visual assessment of LVEF and with quantitative myocardial gated SPECT. The software using learned pattern recognition and artificial intelligence (AutoEF) applied on biplane apical echocardiographic views reduced the variation in measurements without increasing the time required. The method seems to be able to reduce variation in the assessment of LVEF in clinical patients, especially for less experienced readers.

We evaluated a new feature tracking software for its ability to detect infarcted myocardium on cine-MR images. Patients were selected based on the presence or absence of myocardial scar in the perfusion area of the LAD. The software tracked myocardial wall motion and allowed the calculation of velocity, displacement and strain in radial and longitudinal directions. Feature tracking of cine-MR images detected scar segments with transmurality >50% within the distribution of the LAD with 80% sensitivity and 86% specificity (radial strain), without the need for the administration of gadolinium-based contrast.

In summary, we have evaluated some of the noninvasive techniques in the wide array of diagnostic tools available for the diagnosis of ischemic heart disease. Their availability, low costs, freedom from radiation and repeatability are essential as well as their diagnostic ability.

# POPULÄRVETENSKAPLIG SAMMANFATTNING

## (Popular-scientific summary in Swedish)

Vid en obalans mellan syretillgång och syrebehov i hjärtmuskeln uppstår ett tillstånd av syrebrist (ischemi) som om det kvarstår, leder till död av hjärtmuskelceller, hjärtinfarkt. De tidigaste stegen i det ”ischemiska tidsflödet” är oftast tysta för patienten, först senare i förloppet uppträder bröstsmärta. Vid omfattande celldöd påverkas vänster kammares pumpfunktion. Vänster kammares förmåga att pumpa blod är en av de viktigaste prognostiska markörerna för patienter med kranskärlssjukdom. Syftet med denna avhandling var att utvärdera några av de nya oblodiga metoderna för påvisande av ischemi (Delarbete I, II), utbredning av hjärtmuskelskada efter infarkt (Delarbete IV) och reproducibel utvärdering av vänsterkammarfunktionen (Delarbete III).

Nedsatt hastighet och förskjutning (displacement) av hjärtmuskelväggen i vänster kammare är tidiga tecken på ischemi, då de innerst belägna längsgående muskelfibrerna påverkas först av nedsatt kranskärlsflöde. I det första delarbetet utvärderades hur en ultraljudsmetod, pulsad vävnadsDoppler, under provokation av ett ökat hjärtarbete med läkemedlet Dobutamin, kunde påvisa ischemi. Fynden jämfördes med resultat från isotopundersökning av hjärtat (SPECT). Pulsad vävnadsDoppler var användbart och kunde kvantifiera väggrörligheten i vänster kammares längsaxel och metoden kunde skilja mellan patienter med normal hjärtmuskel, ischemi eller infarkt med SPECT. Vi kunde dock inte påvisa inom vilket kärlområde patienten hade ischemi

I det andra delarbetet undersökte vi med kranskärlsDoppler hur mycket det vänstra nedåtstigande kranskärlet kunde öka blodflödet (den s.k. flödesreserven) under adenosin-provokation. Sextionio patienter med klinisk misstanke om ansträngningsutlöst kärlkramp undersöktes med ultraljud i vänster kranskärl och resultatet jämfördes med isotopundersökning av hjärtat. Vi kom fram till att en blodflödeskvot över två i det vänstra nedåtstigande kranskärlet utesluter en förträngning i kranskärlet av hemodynamisk betydelse. En flödeskvot under två är något mer svårtolkad, då ett antal skilda hjärt-, kärl- och ämnesomsättningsriskfaktorer kan bidra till en nedsatt funktion av mikrocirkulationen och av de större kranskärlen. Slutsatsen blev att kranskärlsDoppler under adenosin-provokation är en mycket lovande metod, ffa på grund av att den är oblodig, fri från strålning, tillgänglig och snabb att utföra. Den lämpar sig därför väl till uppföljande kontroller av patienter efter insatt medicinsk behandling mot tex högt blodtryck, höga blodfetter

eller diabetes som ett led i en riskbedömning, men även efter behandling med ballongvidgning av en kranskärlsförträngning.

I det tredje delarbetet fokuserade vi på vänsterkammarens volymer och ejektionsfraktionen, som ett mått på kammarfunktionen. Dessa parametrar är prognostiskt viktiga, varför det är angeläget att de är exakta och reproducerbara. Sextio patienter med misstänkt eller känd kranskärlssjukdom med varierande vänsterkammarfunktion inkluderades i studien. Vi jämförde beräkningar av ejektionsfraktionen utförda med hjälp av en ny datoriserad halvautomatisk utlinjering av den inre hjärtmuskelkonturen (AutoEF) med data från den manuella utlinjering som rekommenderas idag, med visuell skattning av ejektionsfraktionen och med data erhållna från isotopundersökning av hjärtat (Gated SPECT). Data jämfördes mellan erfarna bedömare och nybörjare. Vi fann att den nya programvaran (AutoEF) reducerade spridningen i mätningarna utan extra tidsåtgång. Mest värdefullt var detta för de oerfarna bedömarna.

Utbredningen av kvarstående ärr efter en hjärtinfarkt kan bäst påvisas med en magnetkameraundersökning efter kontrastinjektion med gadolinium. En skada som omfattar >50% av hjärtmuskelväggens tjocklek har små förutsättningar att återfå god funktion även om blodflödet återställs med hjälp av ballongvidgning eller kranskärlsoperation. Detta är ogynnsamt för patienten ur prognostisk synvinkel. I den fjärde delstudien var vår avsikt att utvärdera ett nytt verktyg som följer hjärtmuskelns väggrörelse i kammarens längs- och kortaxel på rörliga bilder registrerade med magnetkamera (cine-MRI), och beräknar dess hastighet, förskjutning (displacement) och deformation (strain). Vi ville undersöka om man med programvaran (Diogenes-MRI) kunde identifiera de delar av hjärtmuskeln som har en skada (påvisad efter gadoliniuminjektion) som omfattar >50% av väggtjockleken. Ur en större studie omfattande 99 patienter valde vi ut 17 patienter med ärr inom försörjningsområdet för vänster kranskärls nedåstigande gren och 13 patienter utan skada inom det området. Vi kunde visa, att med analys av ffa radiell deformation på rörliga MR-bilder så kan hjärtsegment med >50% ärr efter hjärtinfarkt påvisas med hög sensitivitet och specificitet (80% respektive 86%).

Sammantaget har vi utvärderat några av de nyare oblodiga teknikerna som idag finns tillgängliga för diagnostik av kranskärlssjukdom. Vi fann dem användbara och deras gemensamma styrka ligger i metodernas tillgänglighet, kostnadsläge, frånvaro av strålning och att de kan upprepas i uppföljande undersökningar av patienten.

# LIST OF PUBLICATIONS

This thesis is based on the following papers, which are referred to in the text by their Roman numerals.

I Blomstrand, P. **Maret, E**. Ohlsson, J. Scheike, M. Karlsson, J-E. Säfström, K. Swahn, E. Engvall, J. Pulsed tissue Doppler imaging for the detection of myocardial ischaemia, a comparison with myocardial perfusion SPECT.
*Clin Physiol Funct Imaging*, 24(5):289–295 (2004)

II **Maret, E**. Engvall, J. Nylander, E. Ohlsson, J. Feasibility and diagnostic power of transthoracic coronary Doppler for coronary flow velocity reserve in patients referred for myocardial perfusion imaging.
*Cardiovasc Ultrasound*, 6 (12) (2008)

III **Maret, E**. Brudin, L. Lindström, L. Nylander, E. Ohlsson, J. Engvall, J. Computer-assisted determination of left ventricular endocardial borders reduces variability in the echocardiographic assessment of ejection fraction.
*Cardiovasc Ultrasound*, 6 (55) (2008)

IV **Maret, E**. Tödt, T. Brudin, L. Nylander, E. Swahn, E. Ohlsson, J. Engvall, J. Feature tracking of cine-MRI identifies left ventricular segments with myocardial scar.
*Manuscript*

# ABBREVIATIONS

| | |
|---|---|
| ACS | Acute Coronary Syndrome |
| AMI | Acute Myocardial Infarction |
| ANOVA | Analysis of Variance |
| B-A | Bland and Altman |
| BS | Biplane Simpson |
| b-SSFP TFE | Balanced Steady State Free Precession Turbo Field Echo |
| CAD | Coronary Artery Disease |
| CD | Color Doppler |
| CVD | Cardiovascular Disease |
| CMR | Cardiovascular Magnetic Resonance |
| DICOM | Digital Imaging and Communications in Medicine |
| DTI | Color Doppler Tissue Imaging |
| ECG/EKG | ElektroCardioGram |
| FFR | Fractional Flow Reserve |
| ICC | Intraclass Correlation Coefficient |
| IR-TFE | Inversion Recovery Turbo Field Echo |
| IVUS | Intravascular Ultrasound |
| LAD | Left Anterior Descending Artery |
| LBBB | Left Bundle Branch Block |
| LCX | Left Circumflex Coronary Artery |
| LGE | Late Gadolinium Enhancement |
| LV | Left Ventricle |
| LVEF | Left Ventricular Ejection Fraction |
| LVEDV | Left Ventricular End-diastolic Volume |
| LVESV | Left Ventricular End-systolic Volume |
| MAM | Mitral Annular Motion |
| MCE | Myocardial Contrast Echocardiography |
| MPI | Myocardial Perfusion Imaging |
| MRI | Magnetic Resonance Imaging |

| | |
|---|---|
| PCI | Percutaneous Coronary Intervention |
| RCA | Right Coronary Artery |
| ROC | Receiver-operator-characteristics |
| SAX | Short Axis |
| SD | Standard Deviation |
| SPECT | Single Photon Emission Computed Tomography |
| SPSS | Statistical Package for the Social Sciences |
| TR | Repetition Time |
| TTDE | Transthoracic Doppler Echocardiography |
| TVI | Tissue Velocity Imaging |
| WMA | Wall Motion Abnormality |

# INTRODUCTION

## Coronary Artery Disease

The leading cause of death in Sweden, as in the rest of the Western world, is disease of the circulatory system, in men as well as women. In 2006, 42% of all deaths reported had circulatory disease as the underlying cause of death [1] despite advances in medical, interventional and surgical treatments. A century ago the same figure was around 10 %, infectious diseases and malnutrition at that time being the most common causes of death. Although still the leading cause of death, the mortality trend for diseases of the circulatory system has decreased during the period 1987-2006 for both men and women (men from 352 to 146 and women from 128 to 61 deaths per 100.000).

Acute myocardial infarction (AMI) is strongly related to age and gender. The risk for fatal or non-fatal myocardial infarction is twice as high for men than for women in the same age-group. In 2006, the incidence of myocardial infarction in Sweden was 667/100.000 for men and 477/100.000 for women (age 20 years and older). The case fatality has fallen considerably. In 1995, 41% of men and 45% of women died within 28 days after a myocardial infarction, while in 2006 the corresponding numbers were 30% vs. 33%. The somewhat higher mortality in women is mainly related to the fact that they are older than the men when they have their infarct. If the patient is hospitalized the mortality is even lower, 15% for both men and women, average for all age groups.

Left ventricular function is one of the most important determinants for prognosis in patients with coronary artery disease (CAD). Patients with impaired LV systolic function represent a high risk group with significantly higher annual mortality than those with preserved LV function, and survival rates decline in proportion to the severity of dysfunction [2, 3]. In Europe, more than 10 million within a population of 900 million have heart failure. The mean age of patients with heart failure is 70-75 years, almost evenly split between the sexes. In Sweden the prevalence is 2%, but rises with age and affects about 10% of the population older than 80 years. The main causes (80%) of heart failure are chronic hypertension and ischemic heart disease. Heart failure therefore represents a substantial financial and social burden that will continue to grow as successful treatments for previously fatal cardiovascular diseases are implemented.

## Coronary flow, resistance and flow reserve

Myocardial oxygen extraction is near-maximal at rest, averaging 75% of arterial oxygen content [4]. Increases in myocardial oxygen consumption are primarily met by an increase in coronary flow. The major determinants of myocardial oxygen consumption are heart rate, systolic pressure/myocardial wall stress and left ventricular contractility. A twofold increase in any of these individual determinants requires an increase of coronary flow in the range of 50%. Resting coronary blood flow under normal hemodynamic conditions averages 0.7 – 1.0 ml/min/g and can increase more than fourfold during vasodilatation. The ability to increase blood flow above resting values during stress is called coronary flow reserve. Coronary flow reserve is reduced when diastolic filling time is reduced (tachycardia), when preload is increased and by any factor that increases resting flow (i.e. tachycardia, systolic pressure, anemia and hypoxia).

The resistance to coronary blood flow can be divided into three major components: a) the epicardial arteries, b) the microcirculatory resistance arteries and arterioles and c) compressive resistance. The epicardial arteries do not normally contribute to coronary vascular resistance but there are several factors that are able to modulate the arterial diameter, among them paracrine substances, circulating neurohormonal agonists, as well as neural tone and local vascular shear stress. The combined effect of these mechanisms is dependent on whether a functional endothelium is present or not. With the development of an epicardial arterial narrowing (more than 50% diameter reduction) the arterial resistance begins to contribute to the total coronary resistance and when severely narrowed (more than 90%) may reduce resting flow. The microcirculatory resistance vessels, 20-200 µm in diameter are distributed throughout the myocardium and change in response to physical forces (luminal pressure and shear stress) and to the metabolic needs of the tissue. This results in a substantial coronary flow reserve in the normal heart. Compressive resistance varies over time throughout the cardiac cycle and is related to cardiac contraction and systolic pressure within the left ventricle. The effects are most prominent in the subendocardium.

A physiological assessment of the severity of coronary artery stenoses is fundamental in the management of patients with coronary artery disease (CAD). Epicardial arterial stenoses based on atherosclerosis increase coronary resistance and reduce maximal myocardial perfusion. However, in many patients abnormalities in the coronary microcirculatory control also contribute to myocardial ischemia. With angiography the epicardial vessels are visualized, stenoses are quantified and subsequently treated with angioplasty or by-pass surgery when needed. The resistance in the microcirculation is however not influenced by revascularization of the epicardial vessels but by medical therapy.

Gould et al have shown that resting coronary blood flow does not decrease until coronary artery diameter is reduced by 85%. The coronary flow reserve (defined

as the ratio between coronary flow during maximal hyperemia and at rest), however, begins to decrease already with a 30–45% reduction of the arterial diameter [5, 6]. In healthy coronary arteries, adenosine provokes an increase in coronary flow 3–6 times the resting value [7]. Flow reserve can be quantified by intravasal measurements of intracoronary pressure as well as from intracoronary Doppler of flow. A non-invasive method is imaging of tissue perfusion with Positron Emission Tomography (PET), at the expense of using ionizing radiation. A flow reserve below 2 has been shown to be clinically important and to correlate with stress-induced ischemia on SPECT [8]. However, coronary flow reserve is not only influenced by the maximal coronary flow but also by the baseline resting flow value.

## Coronary atherosclerosis and myocardial infarction

Coronary atherosclerosis is a chronic inflammatory disease with stable and unstable periods [9]. Almost all myocardial infarctions result from atherosclerosis, frequently with plaque disruption and thrombosis. Atherosclerosis begins in childhood and progresses over the years but is clinically silent during the early stages. The normal endothelium maintains several vasoactive functions. It produces vasodilatory nitric oxide that counteracts the vasoconstriction that comes from e.g. endothelin. How is the atherosclerotic process initiated? The endothelium does not in general support binding of white blood cells. However, some endothelial cells express selective adhesion molecules on their surface that bind to various classes of leucocytes early after initiation of an atherogenic diet. Fatty streaks and accumulation of extracellular lipids to the intima follow and have been demonstrated mainly at branch points of the arteries. Progressively fibrofatty lesions develop. Ischemic chest pain and an acute coronary syndrome may develop due to plaque expansion and destabilization. When the high-risk fibrous cap disrupts, thrombogenic substances are exposed. That initiates thrombus formation and local production of substances with vasoconstrictor effects (i.e. serotonin, tromboxane $A_2$ and thrombin) that enable vasoconstriction not only locally but also downstream, worsening the ischemic burden.

Myocardial ischemia reflects an imbalance between oxygen supply and demand. Sigwart et al [10] have introduced the concept of the “ischemic cascade”, a sequence of events that occurs when the myocardial blood supply is insufficient for the metabolic demand which can be seen e.g. during balloon obstruction of the coronary artery in humans. After arterial occlusion, the first events are clinically silent but ventricular function becomes abnormal (diastolic relaxation failure followed by systolic contractile failure) with subsequent increase in the left ventricular filling pressure transmitted to the pulmonary circulation, causing breathlessness. Finally, ECG changes develop due to disturbances in the membrane potential and chest pain caused by the accumulation of metabolites, usually as the last event in the evolution of ischemia (Figure 1).

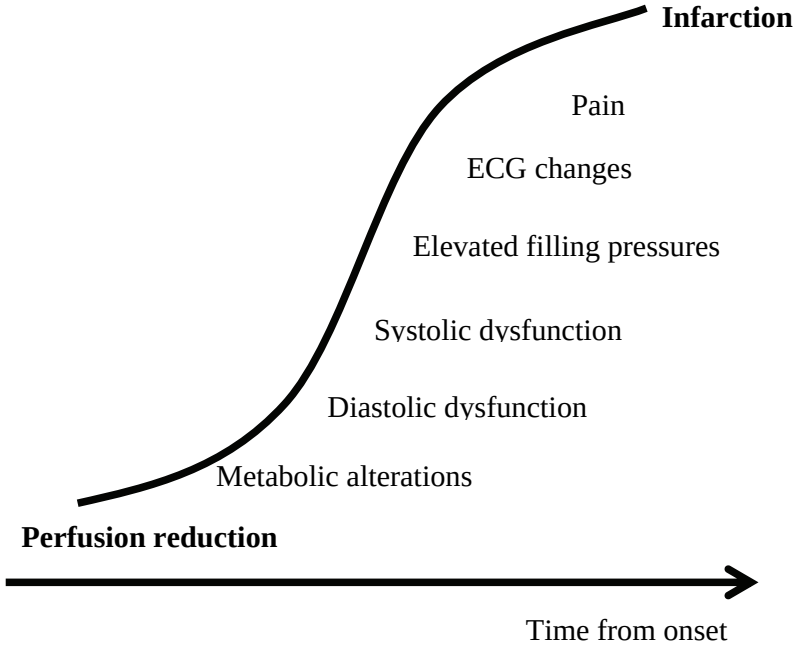


**Figure 1. The ischemic cascade as function of time**

Prolonged ischemia can lead to death of the myocytes, causing myocardial infarction. In the 1970s Reimer and Jennings [11, 12] examined the relation between the duration of ischemia, the area at risk, the collateral blood flow and final infarct size. In their studies on dogs, they showed that the infarct starts at the endocardium and progresses as a wavefront towards the epicardium with increasing duration of coronary occlusion. Coronary occlusion lasting <6 hours resulted in subendocardial damage with a spared epicardial rim but when coronary occlusion exceeded six hours the necrosis became transmural. A collateral network may prevent necrosis from occurring and severe ischemia can therefore be unrecognized/silent to the patient. If ischemia is prolonged, irreversible damage occurs, due to irreversible cell rupture and necrosis despite restoration of myocardial perfusion. When reperfusion of the myocardium occurs early (within 15-20 minutes) it can successfully prevent necrosis from developing even though it may take several hours for contractility to return to normal. Beyond this early stage, the amount of salvaged myocytes/myocardial tissue relates directly to the duration of coronary artery occlusion as well as to the level of myocardial oxygen consumption and the collateral blood flow [13].

## Left ventricular function in coronary disease

The major function of myocardial muscle cells is to execute the cardiac contraction and relaxation cycle. LV systolic function is determined by preload, afterload, myocardial contractility and heart rate. Ejection fraction (measured as [(EDV-ESV)/EDV] x100) is an important parameter of prognostic value, both short and long term, in patients with various heart diseases. Chronic heart failure due to left ventricular systolic impairment is characterized by a very poor prognosis. A five year mortality of 41.5% is significantly higher in these patients than in those with preserved systolic function. However, also patients with heart failure and preserved systolic function have a 25% five year mortality due to abnormal autonomic function [14].

Myocardial blood flow, oxygen consumption and contractile function are tightly linked. In an ischemic area, ventricular function becomes depressed within a few seconds following coronary occlusion. If ischemia is reversed within 10-15 minutes, myocardial function is fully reversible, even though it may take several hours for contractility to return to normal. Four abnormal contraction patterns develop in the ischemic myocardial segment: (1) dyssynchrony, i.e. dissociation in the time course of contraction in adjacent segments, (2) hypokinesis, reduction in the extent of shortening, (3) akinesis, cessation of shortening, and (4) dyskinesis, paradoxical expansion and systolic bulging. A compensatory hyperkinesis of the remaining noninfarcted myocardium can be seen, secondary to increased activity of the sympathetic nervous system that subsides within two weeks following an infarction. With time, edema, cellular infiltration and finally fibrosis increase the stiffness of the infarcted myocardium. If a sufficient quantity of the myocardium undergoes ischemic injury, left ventricular pump function becomes depressed: cardiac output, stroke volume, blood pressure and peak dP/dt decline [15]. Finally, an increase of the end-systolic volume is perhaps the most powerful hemodynamic predictor of mortality following STEMI [16].

Along with the advances in surgical and percutaneous revascularization, studies have shown that LV dysfunction in many patients is a potentially reversible phenomenon and in these patients LV function may improve or even normalize, after revascularization. As many as 40% of patients with depressed LV function undergoing coronary artery bypass surgery manifest a significant increase in left ventricular ejection fraction when evaluated several months after surgery [17-20].

Viable but dysfunctional myocardium has been defined as any region that improves contractile function after coronary revascularization [21]. Even if perfusion is successfully restored, and in the absence of necrosis, regional myocardial contraction can remain depressed at rest, reflecting the development of a post-ischemic stunned myocardium [22]. After short single episodes of ischemia,

myocardial function normalizes rapidly, but if ischemia increases in duration, stunning can be prolonged even though the blood flow has been restored. This is sometimes seen following cardiopulmonary bypass [23-25]. Contractile function that normalizes during stimulation with inotropic agents, displays that the stunned area has contractile reserve. Myocardial stunning requires no therapy, since blood flow is normal, and will usually normalize spontaneously within one week. Stunned myocardium can also be seen after stress- or exerciseinduced ischemia when regional function remains depressed distal to a coronary stenosis, even though perfusion is restored at rest, and after repetitive ischemia (cumulative or chronic stunning).

When myocardial dysfunction is present and resting blood flow is reduced in the absence of signs of ischemia or myocardial infarction, chronic myocardial stunning (normal resting flow) progresses to hibernating myocardium (reduced resting flow) [21]. Both chronic stunning and hibernating myocardium reflect an exhausted coronary flow reserve (Table 1). Rahimtoola suggested in 1985 the definition of myocardial hibernation as: “a prolonged subacute or chronic state of myocardial ischemia . . . in which myocardial contractility and metabolism and ventricular function are reduced to match the reduced blood supply,” which is “a new state of equilibrium . . . whereby myocardial necrosis is prevented, and the myocardium is capable of returning to normal or near-normal function on restoration of an adequate blood supply” [26]. Many patients with hibernating myocardium present with left ventricular dysfunction rather than symptomatic ischemia. Hibernating myocardium is also prone to develop lethal arrhythmias [27]. Although there are well-known limitations in the use of meta-analyses [28, 29], one meta-analysis of 3,088 patients with chronic coronary artery disease and left ventricular dysfunction (LVEF 32±8%), showed that patients with evidence of myocardial viability had a clear benefit from revascularization versus medical therapy in terms of 3.2% versus 16% annual mortality over 25±10 months follow-up [30].

**Table 1. Characteristics of stunning, hibernation and ischemia**

| Parameter | Stunning | Hibernation | True ischemia |
|---|---|---|---|
| **Myocardial function** | Reduced | Reduced | Reduced |
| **Coronary Blood Flow** | Normal/high | Modestly reduced | Most severely reduced |
| **Myocardial metabolism** | Normal/excessive | Reduced/ steady state | Reduced, increasingly severe |
| **Duration** | Hours to days | Hours/days/months | Minutes to hours |
| **Outcome** | Full recovery | Recovery if blood flow is restored | Infarction if ischemia persists |

## Cardiovascular imaging techniques

Clinical decision-making, though central to all patient care, is growing increasingly complex. The array of diagnostic options is escalating, as well as the cost of care. Tests that provide clinical value do so by adding new information to what is already known about the patient. Therefore the cost-effectiveness of a test is determined not only by its information content, but also by its effects on patient outcomes. In clinical decision making, Bayes´ Theorem is highly relevant. Diagnostic tests are mainly used to answer the question: "what is the probability that the patient has the disease given an abnormal test". Bayes´ Theorem relates the change in probability given new information. The test acts as an opinion modifier, as the post-test probability is a function of the pre-test probability and the likelihood ratio (Post-test Odds = Pretest Odds x Likelihood Ratio) [31, 32]. The likelihood ratio is derived directly from the test´s sensitivity and specificity. The only truly useless test result is one with a likelihood ratio of 1.0 (sensitivity and specificity both 50%), because it does not modify the post-test probability. Various diagnostic methods answer the following questions differently depending on the sensitivity and specificity of the method: Given this diagnostic result, what is the post-test probability that my patient has the disease (positive test)? Is this method able to rule out the disease, given this result (negative test)?

| | |
|---|---|
| Sensitivity: | the proportion with a positive test among those with the disease (true positive) |
| Specificity: | the proportion of a negative test among those without disease (true negative) |
| Positive predicted value: | the proportion that has the disease among those with a positive test |
| Negative predicted value: | the proportion that does not have the disease among those with the negative test |
| Likelihood ratio (LR): | the ratio of the probability of a certain test result in people with the disease to the probability in people without the disease |
| LR (positive test result): | sens/(1-spec) |
| LR (negative test result): | (1-sens)/spec |

Clinical decisions also involve balancing the benefit and risk of a diagnostic test. The diagnostic problem to resolve is important. Diagnostic tests are ordered for several reasons: to establish a diagnosis in a symptomatic patient, to screen for disease in an asymptomatic patient, to provide prognostic information in patients with established disease, to monitor therapy but also to establish that a person is free from disease. In all these situations the pre-test probability for disease may be high or low which should influence the diagnostic modality to choose.

Today the physician has an array of diagnostic options with varying advantages and limitations. Some techniques are widely available, easy, fast, mobile, inexpensive, non-invasive and/or non-ionizing, whilst other techniques are time-

consuming, require advanced diagnostic equipment and highly skilled personnel, maybe exposing the patient (and personnel) to ionizing radiation, and therefore costly. In addition, the accuracy and reproducibility of a test influences the diagnostic method of choice. The accuracy of a test is determined by its ability to identify the target disorder/disease compared to a recognized and validated reference test (gold standard). When the gold standard is invasive or uses ionizing radiation, it may in some cases be considered unethical and unacceptable as well as impractical and costly to test patients having a low pre-test probability for a specific disease; given that angiography has a certain risk of morbidity and even mortality and radiation may induce cancer. The diagnostic method of choice must always be the method that exposes the patient to smallest risk given the best possible diagnostic information about the investigated disease regarding the pre-test probability. An important issue in this decision-making should also be if the diagnostic procedure is to be repeated in the future. A procedure that is invasive or utilizes ionizing radiation exposes the patient to a larger risk over time when repeated. In general, ionizing radiation is less dangerous in patients >50 yrs old, but unnecessary radiation of the population should be discouraged.
In the following section we are going to focus on some of the imaging techniques that were used in this thesis.

### Echocardiography

Transthoracic echocardiography is often the first and the most frequently used imaging modality to diagnose and evaluate cardiovascular disease in cardiological practice. In 2003, more than one out of every four imaging study was performed with ultrasound worldwide [33]. It is easily available and mobile (sometimes hand-held), non-invasive, non-ionizing, inexpensive and therefore often used bedside in a clinical unit, as well as in highly complex and expensive research systems. It has the ability to detect structural, functional and hemodynamic abnormalities of the heart.
Cardiac structures and wall motion are visualized in real-time two-dimensional (2-D) and three-dimensional (3-D) echocardiography. The temporal resolution is excellent, about 10-30 ms for 2-D imaging, but substantially lower for 3-D, about 50 ms. Color Doppler displays blood flow direction, velocities and turbulence, superimposed on the 2D image, by encoding the measured frequency shift (see below) of the blood flow at the sampling site into a predefined color scheme. Structural and hemodynamic abnormalities of the heart produce disturbances in the blood flow that are easily recognized. Blood velocities can be measured by pulsed wave Doppler that is localized to a specific region of interest, and continuous wave Doppler, which records all the velocities along the path of the ultrasound beam.
Tissue Doppler Imaging (TDI) is a modified pulsed wave Doppler technique that can measure the motion of myocardial tissue with a frequency shift much lower than that of blood flow, but with a higher amplitude. TDI can also be color encoded.

Contrast echocardiography after intravenously administered inert gas-filled microbubbles that pass the pulmonary circulation, opacifies the left ventricular cavity and enhances the endocardial border. It improves the estimation of left ventricular ejection fraction at rest as well as optimizes regional wall motion analysis during stress echocardiography, and it also enables the assessment of myocardial perfusion [34-36]. Intracardiac and intracoronary transducers [37-39] allow an even higher spatial resolution, a development that has accelerated lately due to demands in interventional cardiology.

The Doppler effect:

Doppler echocardiography measures blood flow velocities on the basis of the Doppler effect (described by Christian Doppler in 1842). In short, the difference in frequency between transmitted sound with a known frequency (fo) and reflected sound waves by the blood cells (fr) is the frequency or Doppler shift ($\Delta f=fr-fo$). The Doppler shift is related to the transmitted frequency (fo), the velocity of the blood cells (v) and the angle between the ultrasound beam and the moving target ($\Theta$). This can be expressed in the Doppler equation as $\Delta f = 2\ fo \times v \times \cos \Theta / c$, where c is the speed of sound, approximately 1540 m/sec in blood. The velocity of blood cells can therefore be calculated as follows: $v = \Delta f \times c / 2\ fo$.

**With special reference to coronary flow reserve**

Measuring the coronary flow reserve allows the detection of early changes causing luminary constriction at the beginning of the ischemic cascade. There are a number of methods for determining coronary flow reserve: coronary angiography with pressure transducer or intravascular Doppler wire (IVUS), positron emission tomography (PET), magnetic resonance and transthoracic ultrasound (TTDE).

Coronary angiography is presently the standard method to assess coronary anatomy. It is an invasive method requiring exposure to radiation and the infusion of a contrast medium. The severity of stenoses is graded visually, a method limited by observer variability and bias [40-42] and gives little information on the physiogical significance of the obstruction. Already in 1992, Doucette and colleges validated intracoronary Doppler guide wire for measuring intracoronary velocities [43]. Today, to identify a culprit lesion, a pressure guidewire is placed distal to the stenosis and the pressure gradient is measured during hyperemic stress produced by adenosine-induced dilatation of the microvasculature, the fractional flow reserve (FFR) [44]. Normal FFR is 1.0 and a lesion is considered significant if the FFR is less than 0.75 [45-48].

PET is a technique utilizing short lived isotopes for the tracking of cellular metabolism and is accepted as the gold standard also for measurements of myocardial flow at rest and during hyperemia [49, 50]. However, the use of this technique is limited by radiation, cost and availability.
MRI is a non-ionizing, non/semi-invasive modality but is limited by cost, availability and the requirement of highly skilled personnel. Contrast-enhanced MRI, using a first-pass technique has been validated in animal studies [51, 52] and the ability to measure absolute blood flow and flow reserve has been introduced [53, 54] and compared to PET flow measurements [55] and to intracoronary Doppler flow wire [56]. Schwitter et al [57] have, in addition, used phase-contrast MRI to assess global coronary sinus blood flow with PET as reference, as a promising tool for studying coronary hemodynamics in generalized diseases of the left ventricle.

Due to better transducers and ultrasound hardware, transthoracic Doppler echocardiography (TTDE) of the distal left anterior descending and right descending arteries has evolved to become a non-invasive, non-ionizing and inexpensive method available bedside for the evaluation of coronary flow reserve (CFVR) [58-62]. CFVR in the distal circumflex artery has been more difficult but not impossible to measure [63]. Introduced in the late 1990s by Voci et al [64, 65], the method is technically challenging due to several problems such as cardiac motion, poorly detectable coronaries, adenosine-induced tachypnea and tachycardia. Okayama et al [66] showed that the administration of an intravenous echocontrast agent may improve the rate of successful CFVR measurements from 70% to 97%. CFVR measured with TTDE correlated with quantitative coronary angiography [67], PET [68] and intracoronary guide wire [69-71].

As discussed earlier, CFVR reflects the severity of total coronary resistance including the patency of the epicardial coronary arteries and the vasodilator capacity of the microcirculation. Therefore, if epicardial coronary arteries are normal, CFVR entirely reflects the resistance of the microcirculation. But the impact of the microcirculation on CFVR is of secondary importance in the presence of a significant epicardial flow-limiting stenosis. As suggested by Gould et al [5, 6], a cut off value of 2 discriminates a significant (≥70%) stenosis from a non-significant (<70%) coronary stenosis, findings that have been confirmed in later studies [72, 73]. The physiologic impact of an intermediate stenosis (50-69%) is difficult to quantify with coronary angiography, but possible to evaluate with CFVR [74], therefore making it a promising tool in clinical decision-making. CFVR measured by TTDE can also be used as a follow-up after percutaneous coronary interventions [62, 75] and to evaluate coronary recanalization in AMI [76, 77]. Studies with CFVR have evaluated endothelial function in diabetes [78], obesity [79], left ventricular hypertrophy [80, 81], dilated cardiomyopathy [82], in endurance athletes [83], cigarette smokers [84] and consumers of red wine [85]. Voci et al report that altered microvascular circulation may decrease

CFVR to not less than 2-2.5 except in patients with syndrome X were CFVR may fall below 2 [86].

Due to its availability and freedom from ionizating radiation CFVR can be repeated over time. Therefore, in experienced hands, it can readily be used to risk stratify a patient with risk factors for developing CAD, or to evaluate treatment, not only regarding the value of CFVR per se, but also to determine if the medical treatment (i.e. anti-hypertensive, lowering cholesterols or the glucose levels) induces an improvement in CFVR-values over time.

Why adenosine as a stressor? Adenosine is a strong dilatator of the coronary microcirculation decreasing mainly peripheral resistance. Therefore, CFVR can be used as a surrogate for coronary flow reserve, which is the product of velocity and the cross-sectional area of the vessel. Sudhir et al [87] showed in their study little effect on the epicardial arteries, but lately Kiviniemi et al have shown that the epicardial coronary arteries increase in diameter up to 31% during adenosine infusion [88, 89]. Adenosine is readily cleared from the blood with a short half-time of 10 sec. Due to the mechanism of the adenosine effect, conduction through the A-V-node is reduced which contraindicates its use in second- or third grade A-V-block and sinus node disease. Adenosine is also a respiratory stimulant and should be avoided in patients with easily induced asthma. The effects of adenosine are antagonized by methylxanthines (i.e. caffeine and theophylline), and potentiated by dipyridamole. The effect of adenosine infusion (140 µg/kg/min) on the microvascular circulation is clearly detectable during TTDE, with a hyperemic phase within 2 minutes after start and a fast return to baseline within a few minutes after stopping the infusion. Dipyridamole, also used by some investigators, inhibits the uptake of adenosine resulting in an increase in local concentrations of adenosine. It therefore also decreases coronary vascular resistance but the onset is slower and the wash-out time longer (up to 3 hours).

**With special reference to wall motion in coronary artery disease**

Immediately after the onset of ischemia, myocardial perfusion, diastolic dysfunction and contractility become abnormal, before other clinical manifestations, such as ECG-changes or chest pain. Echocardiography at rest can detect these changes, but is not sufficient to evaluate the cardiovascular reserve capacity of the heart that is needed for proper adaptation and function at more stressful conditions. Therefore, the possibility to stress the heart with exercise or with a pharmacological agent is extremely valuable since it allows the simultaneous evaluation of myocardial perfusion, wall motion, changes in filling pressures, valvular regurgitation and pressure gradients, in comparison with conditions at rest. Exercise test (supine bike or treadmill test) is preferred for the evaluation of valve disease and pharmacological test when coronary artery disease is evaluated, i.e. myocardial ischemia and viability and as a part of preoperative risk stratification.

Intravenous infusion with Dobutamine in three-minute stages of stepwise elevation in infusion rate, is the most frequently used technique, due to its direct-acting inotropic (mainly during low dose infusion, ≤10 μg/kg/min) and chronotropic effect (stimulation of β-receptors of the heart). The drug has, however, also hypertensive and arrythmogenic effects and decreases peripheral vascular resistance which can cause premature interruption of the study. The plasma half-time in humans is 2 minutes, which enables its use in an outpatient clinic setting. By adding atropine (0.2-1.0 mg) in the final stage of dobutamine-stress (40-50 μg/kg/min), more patients reach the target heart rate (85% of 220-age) to enhance the sensitivity of the test. When assessing myocardial perfusion at stress, adenosine or dipyridamole is used more frequently. Due to their vasodilating effects, leading to a "vascular steal", myocardial segments perfused by a stenotic coronary artery reveal a decrease in the regional myocardial perfusion. Myocardial contrast echocardiography (MCE) during dipyridamole stress is valuable as a risk stratification tool, because it reveals perfusion abnormalities preceding wall motion abnormalities in the ischemic cascade. MCE has been shown to be a rapid and safe bedside method [90] comparable with SPECT in detection of CAD [91] and even superior to SPECT for patients with a medium pretest probability of CAD [92].

During dobutamine stress echocardiography (DSE) regional wall motion of the left ventricular segment is evaluated from the parasternal and apical views. Wall motion in each segment is visually estimated on the basis of its contractility and a wall motion score index (WMSI) is calculated.

| Visual assessment of wall motion: | |
|---|---|
| 1: | normal (>40% thickening with systole) |
| 2: | hypokinesis (10-30% thickening) |
| 3: | severe hypokinesis or akinesis (<10% thickening) |
| 4: | dyskinesis |
| 5: | aneurysm |
| WMSI: | sum of wall motion scores/number of segments visualized |

A normally contracting left ventricle has a WMSI=1, but the score increases as the wall motion abnormalities become more severe. Visual assessment of wall motion relies on experience [93] and knowledge of the limitations of the method that may over- and underestimate wall motion; such as translation of the entire heart through the echocardiographic beam, tethering of adjacent segments and underestimation of wall motion of adjacent segments to a hyperkinetic segment. Hoffman et al [94] has shown good agreement between expert readers at five different echocardiographic centers in patients with triple vessel disease, but only 59% agreement in patients with single vessel disease. In comparison with

SPECT, the two methods have similar sensitivity (85% and 87% respectively) but somewhat higher specificity (77% and 64% respectively) [95].

An alternative approach to the diagnosis of subendocardial ischemia is to measure the velocities of regional longitudinal function of the left ventricle from the apical windows using pulsed tissue Doppler imaging. Derumeaux et al [96] showed that already within 15 seconds after the onset of LAD occlusion, there was a significant fall in the maximal velocity of systolic contraction, as well as the velocity during isovolumetric contraction and the early diastolic velocity in the basal septum, measured from apex.
The sampling of peak systolic velocities can be made in real-time in segments during the standard stages of the stress protocol but an alternative and more appealing approach is to record all data as a high frame rate color Doppler data set for later post-processing. The highest possible sampling rate should be achieved, not less than 100Hz (optimal frame rate is >150 Hz), because a too low frame rate could underestimate the maximal velocities and isovolumetric time intervals. The depth of field and the sector angle should be kept at a minimum to achieve the highest possible frame rate.
A weakness in the method is its reproducibility. The variability of pulsed tissue Doppler for on-line measurements of peak systolic velocities has been reported to 20% [97]. In the MYDISE-study [98], the inter-observer variability for off-line measurements of peak systolic velocities in the basal segments was assessed to 10% (coefficient of variation) that is feasible, but almost 50% in the apical segments. The interobserver variability was even higher for the diastolic velocities and isovolumetric times.

## Cardiovascular Magnetic Resonance

Cardiovascular magnetic resonance (CMR) is an established diagnostic modality demonstrating supreme image quality, high spatial resolution, and good reproducibility. Its non-invasive and non-ionizing properties, combined with the continuously ongoing technical advances, have allowed more frequent use and new insights into cardiovascular morphology and function. However, availability is comparatively restricted due to costs and need for highly skilled staff. Currently, 1.5 T magnets are most frequently used, but some institutions use 3 T magnets, also for clinical cases.

Basic MR physics:

The physical interaction is at the level of the nucleus. Because MR does not interfere with electrons in the outer layer or interact with electron binding, it is safe. Magnetic resonance occurs in atomic nuclei with unpaired nuclei. The nuclei most suitable for clinical MR investigation is $^{1}H$, which has a high natural abundance in the human body (water and fat). Hydrogen nuclei behave like magnets and align to an external magnetic field. At baseline, the nuclei spins randomly parallel to the field (low energy state). When the body is excited with a radio frequency pulse, the excited nuclei rotates away from (anti parallel to) the main magnetic field axis (the flip angle) into a higher energy state, which causes a net magnetization. After the excitation pulse is finished, the nuclei relax to their former position and the energy is transmitted to a radio signal. This signal is formed to a radio wave echo and interpreted into an image. Due to different delay between excitation and signal readout (echo time, TE) and between the repetitive radio wave excitations (repeat time, TR), different tissues can be emphasized in the image. By changing the relaxation times in the longitudinal axis (T1) and transverse axis (T2) different biological tissues can be visualized. An additional gradient field, which can be switched on and off, can be used to localize the radio waves coming from the body [99].

CMR has a central role in the diagnosis of cardiovascular disease due to its ability to define anatomy, to characterize properties of tissue, assess function of myocardum and valves, as well as angiographically visualize vessels and flow. Therefore, it has a given place in the investigation of patients with coronary artery disease, congenital heart disease, valve disease, cardiomyopathies, myocarditis, diseases of the great vessels, and cardiac/paracardiac masses. Due to its interstudy reproducibility [100], CMR is very suitable to use in follow up studies. The principal contraindications of the MRI procedure are mostly related to the presence of metallic implants in a patient, such as cardiac pacemakers, automatic cardioverter defibrillators, and ferromagnetic haemostatic clips in the nervous system or metallic splinters in the eye.

**With special reference to delayed enhancement imaging and myocardial viability**

In acute ischemia, myocardial edema is visible with T2-weighted spin-echo-technique. To identify scar tissue after myocardial infarction, application of an intravenous contrast agent is necessary. Gadolinium (named after the Finnish chemist and geologist Johan Gadolin, 1760-1852) is a paramagnetic metal suitable for intravascular and extracellular enhancement of the MR signal by shortening T1. Intravascular (also called non-diffusible) agents have prolonged blood residence (>1 hour) compared to extracellular agents <20 minutes). The extracellular agents distribute into intercellular space but not into intact cells. Due to cell rupture and necrosis of the myocytes, the extracellular volume increases and thus the distribution of the contrast agent, leading to altered wash-in and wash-out kinetic [101]. Kim et al [102] showed an excellent agreement of infarct location and size with this technique related to histology in a canine model. The enhancement technique is highly reproducible [103] and correlates well with SPECT [104] and PET [105]. The higher the transmural extent of gadolinium enhancement (scar), the lower the functional recovery after revascularization, the threshold seems to be about 50% transmural enhancement [106]. In dysfunctional segments with transmurality between 25-50%, the likelihood of improvement is approximately 50%. A low-dose dobutamine stress test to evaluate the inotropic reserve may improve the diagnostic accuracy [107].

Myocardial perfusion single photon emission computed tomography

Noninvasive radionuclide cardiac imaging began in the early 1970s. The most commonly used procedure is single-photon emission computed tomography (SPECT) imaging of perfusion. Following the injection of the radiotracer, the isotope is extracted from the blood by viable myocytes and retained in the cell. Photons are emitted from the myocardium in proportion to the uptake, that is related to the perfusion. The nuclear detector captures the gamma ray photons, and converts the information to digital data. A collimator attached to the gammacamera selects photons that are parallel to the collimator holes, allowing localization of the source of emitted gamma rays. The collected data represents magnitude and location of uptake, thus the distribution of perfusion throughout the myocardium.

The first clinically used tracer was Thallium-201, with a half-life of 73 hours. First pass extraction fraction is high 85%, and peak myocardial concentration occurs within 5 minutes of injection.
In the 1990s Technetium 99m-labeled tracers were introduced. Tc-99m emits 140 keV of photon energy and has a half-life of 6 hours. Two 99m-labeled tracers, sestamibi and tetrofosmin, are approved for clinical use. They are lipid-soluble cations, with first pass extraction fraction of 60% and minimal redistribution.

They are retained within the mitochondia after crossing the sarcolemma and mitochondrial membranes by passive diffusion.

The quality of a study is dependent on adequate provocation, calibrated equipment, absence of patient movements, awareness of possible attenuation artifacts (breast, obesity, abdominal structures etc.) and zones of increased activity (e.g. liver, bowel). Today, interpretation of a SPECT study is a combination of visual analysis and computer-aided quantitative analysis.

To assess ventricular function and calculate ejection fraction, the patient´s ECG is monitored simultaneously, gated SPECT. The R-R- interval is divided into a prespecified number of frames and images are recorded during these time intervals separated from each other. Each timeframe thus represents a time interval of the cardiac cycle as an average of the beats recorded. If the R-R-interval is inhomogeneous, as in atrial flutter or frequent ectopic beats, many beats are rejected leading to a lower accuracy. Left ventricular volumes and calculated ejection fraction calculated with gated SPECT in patients with CAD have been shown to have prognostic value [108-110].

Assessment of infarct size (fixed defects) with SPECT has been validated against other modalities, and also used as a prognostic tool [111-113]. In myocardial perfusion imaging (MPI) with SPECT imaging, relative differences of tracer uptake in stress and rest, can be detected and quantified. Regions with stress-induced perfusion defects that have normal perfusion at rest represent viable regions with blunted coronary flow reserve. In an attempt to summarize data from a total of 33 studies, sensitivity to detect CAD was 87% (range 71-97%) and specificity to rule out CAD was 73% (range 36-100%) [114], with no difference between exercise and pharmacological stress testing. Few had incorporated gated SPECT and attenuation correction, therefore an underestimation of the specificity may have been made. Exercise stress to induce coronary hyperemia, gives additional information on symptoms during exercise, exercise duration and achieved workload together with ECG changes. These are important diagnostic and prognostic factors. When a patient is incapable of achieving sufficient workload, pharmacological stress with adenosine, dipyridamole or dobutamine can be used [115].

# AIMS

The general aim of this thesis was, following the path of the ischemic cascade, to evaluate the feasibility of new non-invasive techniques for the detection of myocardial ischemia, for the identification of the extent of infarcted myocardium and for the quantification of systolic left ventricular function.

The specific aims for each study were:

- to prospectively compare the longitudinal myocardial peak systolic velocity, assessed with pulsed tissue Doppler during dobutamine-atropine stress, with perfusion abnormalities at exercise stress myocardial perfusion SPECT, for the identification of myocardial ischemia (Paper I)

- to evaluate the diagnostic ability of transthoracic Doppler echocardiography in the left anterior descending coronary artery to that of myocardial perfusion imaging (MPI) in an unselected population of patients with chest pain referred for MPI (Paper II)

- to evaluate an automatic computerized algorithm using an adaptive appearance model of the left ventricle with conventional echocardiographic methods to estimate left ventricular volumes and ejection fraction in clinical practice (Paper III)

- to use a new feature tracking software on cine magnetic resonance images to evaluate its utility and ability to detect infarcted myocardium and to assess the transmural extent of scar without the need for administering intravenous gadolinium-based contrast agents (Paper IV)

# MATERIALS AND METHODS

## Patients

All studies complied with the Declaration of Helsinki and with agreements on Good Clinical Practice. Approval was obtained by the Regional Ethics Committee of Linköping University (Paper I-II) and by the Regional Ethical Review Board in Linköping (Paper III-IV). All subjects gave informed consent.

### Paper I

Twenty-six patients, 22 men and four women, were investigated as a part of the Fast Revascularization during InStability in CAD (FRISC II) multicentre trial [116]. Inclusion criteria were symptoms of ischemia that were increasing, occurring at rest or suspicious of acute myocardial infarction. Only patients randomized to the non-invasive regime were included. Dobutamine echocardiography and myocardial perfusion SPECT were performed 5–10 days after the unstable episode, 0–3 days apart. At the time of the investigations, all patients were in sinus rhythm and clinically stable.

### Paper II

Sixty-nine patients referred for myocardial perfusion imaging because of suspected or known CAD (44 men, 25 women) were enrolled. Eighteen had a history of a previous myocardial infarction and 14 were revascularised (9 with PCI and 5 with CABG). One patient had an aortic valve prosthesis. Sixty-six patients were in sinus rhythm, two in atrial fibrillation and one had a pacemaker. Twenty-three patients had a normal electrocardiogram. Twenty-two patients had antihypertensive treatment and 11 were diabetics. No changes in medication were made prior to the study. Exclusion criteria were acute myocardial infarction, unstable angina, 2nd degree AV-block or higher, obstructive pulmonary disease or treatment with dipyridamole as well as theophylline preparations. The subjects were instructed to abstain from xanthine-containing food and drinks (chocolate, cola, coffee and tea) for at least 24 hours before the study.

### Paper III

Sixty patients, 19 women and 41 men, with known or suspected coronary artery disease scheduled for MPI, were enrolled. All patients were in sinus rhythm, which, however, did not constitute a criterion for inclusion. Twenty-four had a history of previous myocardial infarction and 28 had earlier been revascularized.

The only exclusion criterion was unwillingness to participate in the study. One patient had to be excluded due to technical problems with the images. Pharmacologic treatment was held constant. For each patient two-dimensional echocardiography was performed within one hour of MPI at rest.

Paper IV

The study population was selected from 99 patients included in a study of primary PCI for ST-elevation myocardial infarction. These patients agreed to return for infarct size determination with MRI 6±2 weeks after primary PCI. Thirty patients, 3 women and 27 men, were selected based on the presence or absence of extensive myocardial scar in the perfusion area of the left anterior descending coronary artery but not in remote areas. Seventeen patients with scar transmurality >75% in at least one segment belonging to the LAD area (scar patients) and thirteen without scar in this area or in any other parts of the myocardium were selected (non-scar patients). Three patients in the scar group had a history of previous myocardial infarction. Two of these had undergone PCI in addition to one patient in the non-scar group. None of the patients had been subjected to CABG. Initial exclusion criteria were unwillingness to participate in the study or those related to performing MRI such as pacemaker, atrial fibrillation or claustrophobia. Pharmacologic treatment was held constant.

## Echocardiography

### Dobu-stress and Tissue Doppler Velocity (Paper I)

2D echocardiography and pulsed tissue Doppler were performed with the subjects in the left lateral position at rest and during the dobutamine infusion, beginning with the 2D images followed by the tissue Doppler recordings. Images were obtained using a 128XP/10c echocardiograph (Acuson, Mountain View, CA, USA) with a V4C probe. The recordings were stored on videotapes. Dobutamine was administered intravenously beginning at 5 μg $kg^{-1}$ body weight $min^{-1}$ increasing stepwise every sixth minute to 10, 20, 30 and 40 μg $kg^{-1}$ $min^{-1}$. Intravenous atropine (0.25 mg every 1 min up to a maximum of 1 mg) was injected at peak dose dobutamine, when necessary to achieve >85% of the patients age-predicted maximal heart rate (220-age). A 12-lead electrocardiogram was continuously recorded before, during and up to 6 min after the dobutamine infusion was discontinued. Blood pressure was determined by the auscultatory method at rest and during the infusion at 2–3 min intervals. Preset criteria for stopping the infusion before peak-dose were: (1) >2 mm ST-segment depression on the electrocardiogram in a lead with normal ST-segment at rest, (2) significant side effects or arrhythmia, (3) achievement of 85% of the age-predicted maximal heart rate (220-age), (4) new stress induced wall motion abnormalities involving two or more segments, (5) strong chest pain, (6) decrease in systolic blood pressure >30 mmHg or a systolic blood pressure <100 mmHg. Two-dimensional echocardiography was performed using six standard views (apical two- and four-chamber views, apical long-axis view, parasternal long-axis, and short-axis views at the levels of the papillary muscles and mitral chordae) at baseline and at each step of dobutamine. All cineloops were analysed independently by two experienced observers. The left ventricle was divided into 16 segments for analysis: four segments for the apex and six segments for the basal and six for the middle level [117]. The wall motion of each segment was classified according to a 6-grade scale; 0, not visualized; 1, normal; 2, hypokinesia; 3, akinesia; 4, dyskinesia; and 5, aneurysm. Echocardiograms were interpreted without knowledge of clinical data or tissue Doppler results. When there was a disagreement about the result, the two observers together reviewed the study and reached a consensus on the grading.

The Doppler programme was set to the pulsed mode with a sample volume of 4 mm. Filters were set to exclude high frequency signals. Tissue Doppler was recorded at baseline and at each dobutamine level by placing the sample volume at the midwall portions of the basal and middle part of septum, lateral-, posterior- and anterior walls from the apical four- and two- chamber views. Recordings of five to ten cardiac cycles were acquired and the peak systolic (Vs) velocities of three consecutive cardiac cycles were measured and averaged off line by one experienced investigator who was blinded as to the other results.

Coronary Flow Velocity Reserve (Paper II)

Adenosine was administered intravenously (0.140 mg/kg/min) for 5 minutes. A 12-lead ECG was continuously recorded before, during and up to 5 minutes after the adenosine infusion. Blood pressure was determined at rest and at 1–2 minutes intervals during the infusion. Preset criteria for reducing or stopping the infusion were acute bronchospasm, advanced AV block, decrease in systolic blood pressure > 20 mmHg or patient refusal. The examinations were performed with a Sequoia C256 or 512 (Siemens Acuson, Mountain View, California) using a broadband transducer (3V2c and 4V1c respectively). For color Doppler (CD) flow mapping, the velocity range was set at 12 to 20 cm/s. The color gain was adjusted to provide optimal images with minimal "bleeding" of color onto tissue. Coronary flow velocity was measured with pulsed wave Doppler at 3.5 MHz using CD as a guide. Gate size was set at 4–5 mm. Angle correction was performed if the angle between the CD flow and the Doppler beam exceeded 20 degrees and was maintained during rest and stress studies. The spectral trace of the coronary flow was characteristically biphasic with a dominating diastolic component. Stop frames and clips were digitally recorded for off-line analysis. The aim was to record flow in the most distal part of the left anterior descending artery (LAD). To image the distal LAD, the transducer was positioned either at the cardiac apex or one intercostal space above and focused on the proximal field. The transducer was rotated and tilted until the distal coronary segment could be visualized by CD at the epicardial part of the anterior wall (Figure 2). Alternatively, a short axis view of the left ventricular apex and anterior groove was interrogated with CD. When diastolic CD blood flow was detected, the transducer was slowly rotated clockwise to obtain the best long axis view of the LAD. If no CD blood-flow from the LAD was visualized in the baseline condition before the infusion, a new resting recording was made at least 5 minutes after the infusion was stopped. No contrast agent was used. Stop frames of the spectral Doppler signal were repeatedly stored during the investigation (Figure 3a and 3b). Each study was analyzed off-line. Measurements were performed by tracing the contour of the Doppler signal on the ultrasound monitor. Signals with a well defined outline were analyzed and diastolic peak velocities, mean diastolic velocities and diastolic velocity time integrals were measured at baseline and peak hyperaemic conditions. Due to systolic movements of the heart, the systo-diastolic averaged peak velocity and velocity time integral were not always determined. The measurements were, if possible averaged over three consecutive heart beats. Coronary flow reserve was calculated as the ratio of peak hyperaemic and basal mean diastolic velocities.

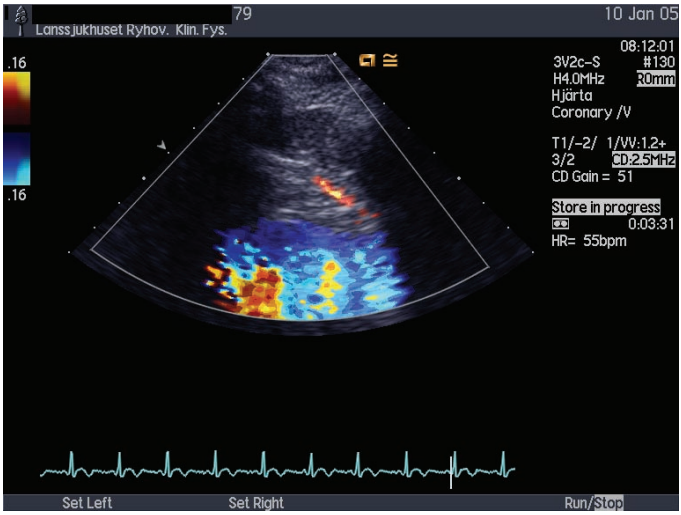


**Figure 2. Color Doppler recording of LAD flow.**

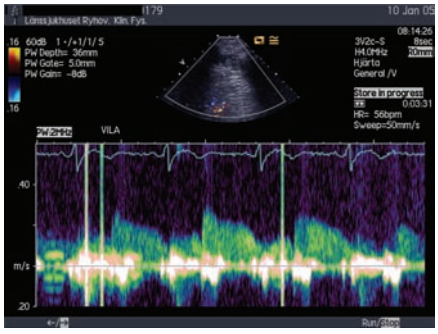


**Figure 3a. Spectral Doppler recording of the LAD flow at rest**

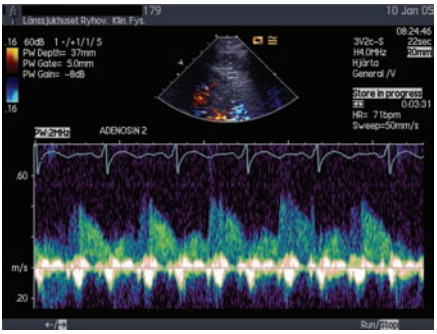


**Figure 3b. Spectral Doppler recording of the LAD flow during stress**

.

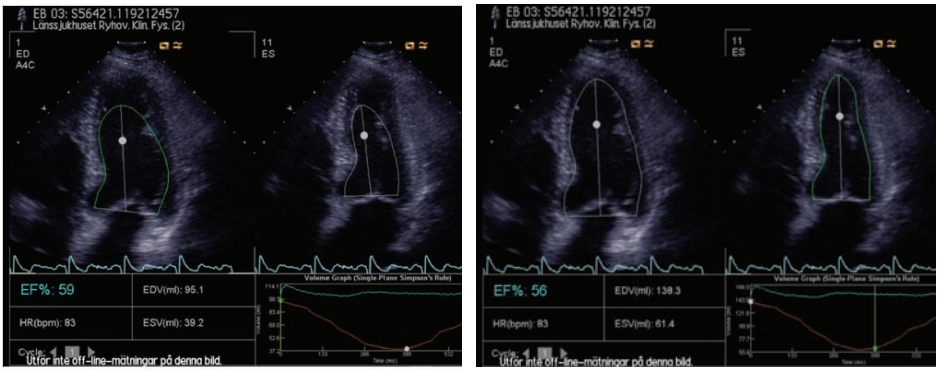


**Figure 4. AutoEF before and after manual correction.**

Left: four-chamber view with automatic delineation of the endocardial border in diastole and in systole by the software. Right: the same images after manual correction of the endocardial border by the operator. This is an example of underestimation of the length of the longaxis of the left ventricle by the software.


**Figure 5. AutoEF without the need for manual correction.**

Four-chamber view with automatic delineation of the endocardial border in diastole and in systole by the software. This is an example of a patient study that did not need manual correction.

AutoEF (Paper III)

Ejection fraction and left ventricular volumes were determined with three echo-based methods and MPI. Five experienced readers (two certified by the accreditation procedure of the European Association of Echocardiography) and two novice readers (cardiology fellows early in their echo-training) were asked to quan-

tify LVEF in each patient using three methods: (1) manual biplane Simpson (manual Simpson), (2) by applying the automatic software (AutoEF) in two apical orthogonal planes, with manual correction if needed (corrected AutoEF), figure 4, and (3) visual assessment of LVEF(%) in four different categories (see below). In addition, one investigator analyzed all studies without manually correcting the delineation by the AutoEF software (uncorrected AutoEF), figure 5. Ten patients were randomly selected for assessment of intra- and interobserver variability. These patient studies were included twice, at random, in the studylist, to avoid bias. All images were anonymized. For measurements, anonymized DICOM-images were reloaded on the scanner, where manual Simpson and corrected AutoEF were performed. The image quality (sharpness of the endocardial border) as well as an estimation of ejection fraction was assessed visually.

The time required for analysis of LVEF using the three methods was recorded. For both AutoEF analyses, the clock was started when the software was activated and stopped when the study report was opened and printed. For biplane Simpson, the clock was started when the study was opened and stopped when the print button was activated.

Study anonymization was repeated between sessions that took place with a three week interval in order to minimize investigator bias. All investigators were blinded to the results of the isotope study.

Echocardiographic imaging was performed by four experienced operators (three technicians, one physician) with a Sequoia C512 (Siemens Acuson, Mountain View, California) using a broadband transducer (4V1c) operating in harmonic imaging mode. Clips of three consecutive beats in the apical 4-, 2- and 3-chamber views were stored digitally. The most representative beat in each view was selected for each patient. Image quality, defined as the extent of visualization of the endocardium, was assessed by the readers in three groups: excellent (1), when all 12 segments of endocardium from the two views were seen, suboptimal (2) when 1–3 segments and poor (3) when 4 or more segments were insufficiently visualized.

Left ventricular function was also visually assessed in four categories: normal (EF > 55%) (1), mildly impaired (EF 45– 54%) (2), moderately impaired (30–44%) (3), and severely reduced (< 30%) (4) [118].

## Magnetic Resonance Imaging

MR exams were performed on a Philips 1.5T Achieva scanner (Philips Healthcare, Eindhoven, the Netherlands). A circular polarized body-array surface coil was used in all measurements. ECG-triggered MR images were obtained during repeated breath holds.
Cine-MRI was performed with a standard b-SSFP TFE sequence and attempted to cover the entire left ventricle with on average 19 (range 17-25) short-axis slices and three long axis planes (2- and 4- chamber views as well as the apical long-axis view). Slice thickness was 10 mm and slice gap -5 mm (i.e. slices were overcontiguous). Temporal resolution ranged between 26-41 ms (30 acquired phases). The contrast enhanced images were acquired at the same slice positions as the cine-images, about 20 min after the administration of Gadopentate dimeglumine (Gd-DTPA) 0.2 mmol/kg bodyweight (Schering Nordiska AB, Järfälla, Sweden). The IR-TFE sequence was a segmented 3D spoiled gradient echo sequence with TE = 1.3 ms, TR= 4.4 ms and TFE factor 43, leading to an acquisition phase time of 188 ms acquired during diastole.

Left ventricular enddiastolic and endsystolic volumes as well as ejection fraction were determined from the cine short axis loops on a stand-alone workstation (View Forum, Philips Healthcare, Eindhoven, the Netherlands) while analysis of velocity, displacement and strain was performed with the feature tracking software (Diogenes-MRI, Tomtec GmbH, Unterschliessheim, Germany) using a standard laptop computer. The apical 2- and 4-chamber views as well as the apical longaxis view were used, after conversion of the DICOM image stack to avi-files. Myocardial scar was visualized with the late gadolinium enhancement technique. Infarct size was determined in milliliters and as a percentage of left ventricular mass, using a computer freeware (“Segment”, www.medviso.com). Infarct transmurality was determined in 19 segments of the myocardium in 3 apical views (3 x 6 plus one apical cap) using the same software (Figure 6). Transmurality was in this setting defined as infarct area divided by segment area and expressed as a percentage. A scar segment was defined as any segment with transmurality >1% (small areas of “scar” may be caused by imperfect segmentation of e.g. the ventricular cavity).

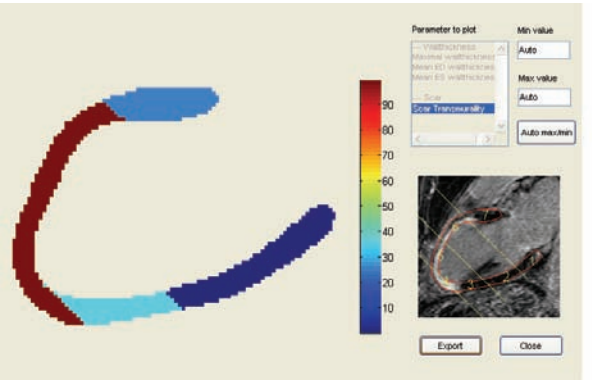


**Figure 6. Transmurality of scar calculated from LGE image in the 2-chamber view**

Scar is 100% transmural along the middle and apical part of the anterior wall extending to the apical part of the inferior wall. MRI with enhanced gadolinium uptake is shown in the box to the right. Calculation was performed with the Segment software.

### Feature Tracking with Diogenes-MRI (Paper IV)

After manually delineating the endocardium and epicardium in diastole, the software tracked the motion of the wall through the entire cardiac cycle using two different techniques, one for edge tracking and the other one using several steps for myocardial pattern recognition successively reducing the uncertainty in the estimation of the position of the pixels (Figure 7). Velocity, displacement and strain were calculated in 48 points (tangential to the endocardial outline, assumed positive in the base-to-apex direction), and in the radial direction (perpendicular to the tangent, positive inward). The left ventricular wall was divided into 6 segments in each of the three views (in pairs at each level, base-mid-apical), giving a total of 18 segments (Figure 8). To allow comparison with the 17 segment model recommended by the American Heart Association [119], two apical segments were added and the top 17th segment fused with the apical segments. The highest systolic value in each segment was used regardless of the presence of a higher postsystolic peak. The tracing of the myocardium was repeated three times and the mean value of the functional measurements was used. In addition, the software calculated a mean value for the six segments in each view and for each parameter. Single-plane left ventricular ejection fraction was reported in each view and an average was calculated from the apical 2- and 4-chamber view for each patient. Global measures were calculated for all parameters as an average value from the three apical views, including all 18 segments.

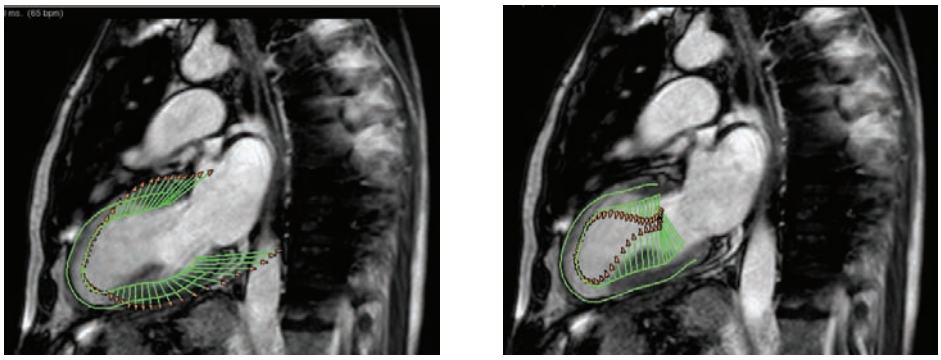

**Figure 7. Velocity vectors from 2-chamber view of the left ventricle.**

Diastolic expansion (left image) and systolic contraction (right image) shows absence of motion in the apex. Same patient as in Figure 6.

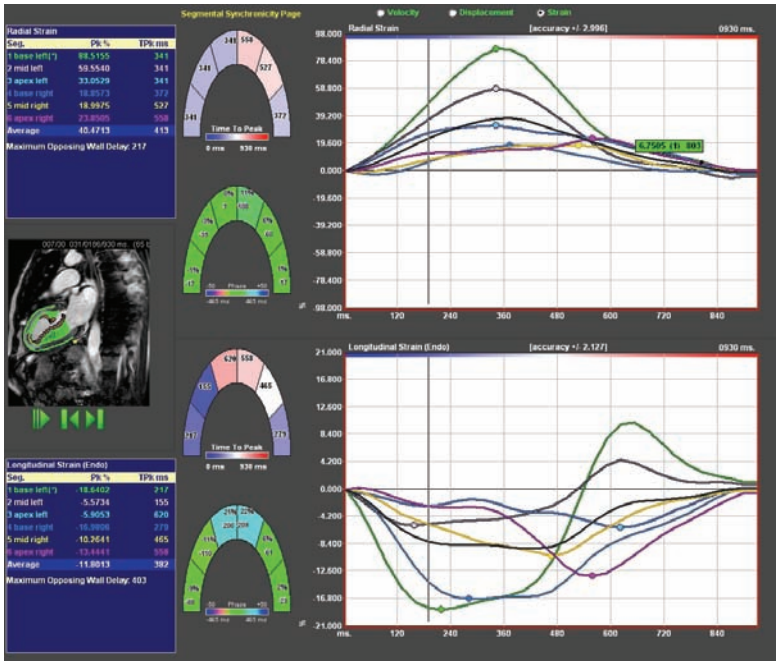


**Figure 8. Measurement window of feature tracking software**

Middle figures show graphical display of 6 segments, three anterior and three inferoposterior. Right upper panel shows radial strain tracings from the six segments. Lower right panel depicts the corresponding longitudinal strain values. Velocity and displacement can be selected for alternative presentation. Left blue box shows peak values (upper left) and time to peak for corresponding segments (lower left).

## Myocardial Scintigraphy

### SPECT (Paper I)

A 2-day exercise/rest SPECT myocardial perfusion protocol was performed. Five MBq Tc-99 m tetrofosmin/kg body weight was injected intravenously 1–2 min before anticipated maximal workload during bicycle exercise. Image acquisition was initiated approximately 15 min later. Rest images were obtained 1–3 days later using 7 MBq Tc-99 m tetrofosmin/kg bodyweight. A single-head Picker SX-300 gamma-camera (Picker International Inc, Ohio, USA) and a single-head GE STARCAM 3000XR/T (General Electric, Reading, UK) equipped with general-purpose parallel-hole collimators were used. Acquisition began in 45° left posterior oblique view with rotation 180° through an anterior arc using 32 projections at 45 s per projection. A 20% window centred on the 140-keV peak was used during imaging. A 64 x 64 word matrix was used with the Picker camera and a 128 x 128 word matrix with the GE-camera. The images were reconstructed using filtered back-projection (Butterworth filter) and resulting slices were re-oriented perpendicular to the heart's long axis. Attenuation correction was not performed. A semiquantitative visual analysis was performed using a 13-segment model. Each segment was classified according to a 4-grade scale: 1, normal uptake; 2, mild defect; 3, moderate defect; and 4, severe defect by the consensus of two experienced observers without knowledge of exercise test or tissue Doppler results. A summed stress score was obtained by the subtraction of 13 from the added scores of the 13 segments. A summed rest score was calculated in the same way. The summed difference score was calculated as the difference between the summed stress and rest scores. According to the summed scores for the stress and rest images, the patients were divided into three groups.

### Gated SPECT (Paper II and III)

Gated myocardial SPECT was performed using a two-day stress/rest protocol. Rest images were obtained using 8.6 MBq 99mTc-tetrofosmin/kg bodyweight. Supine gated SPECT images were acquired 45–60 minutes after the injection. The acquisitions were made on a dual-detector gamma camera (ECAM Siemens Medical Systems Inc) with a low energy high resolution collimator using 64 projections over 180° (right anterior oblique 45° to left posterior oblique 45°), 30 s per projection. A 19% window was asymmetrically placed (129–155 keV) on the 140 keV peak, asymmetry 2%. The gated and ungated data were separately reconstructed on a Hermes Medical Solutions (Stockholm, Sweden) workstation. Prefiltering with a Butterworth filter (cut off 0.8/cm, order 10) was applied followed by filtered back projection. No scatter- or attenuation correction was applied. The reconstructed transaxial images were manually realigned along the cardiac long axis. In Paper III the short axis slices at rest were processed with the

automatic software package QGS (Cedars-Sinai Medical Center, Los Angeles, CA, USA) to calculate LV volumes and global LVEF.

In Paper II adenosine was infused continuously for 5 minutes. Three minutes into the infusion, Tc-99m tetrofosmin was injected and gated SPECT images were acquired 45–60 minutes later. Rest images were obtained 3–5 days later as mentioned above. The reconstructed images at stress and rest were interpreted separately by 2 experienced physicians without knowledge of the outcome of the TTDE. Each observer classified the studies as normal, probably normal, equivocal, probably abnormal and abnormal. In case of an equivocal result, the gated study was evaluated in cine mode, enabling reclassifying the study as either probably normal or probably abnormal. Finally, the normal and probably normal studies were grouped together as were the probably abnormal and the abnormal studies. The perfusion defects were also assigned to LAD, LCX and/or RCA territories. In three cases there was disagreement between the two observers and consensus was negotiated. The "Summed Stress Score" as a measure of perfusion abnormalities was also quantitatively analysed with the software package commonly used at our department (QPS Cedars Sinai, Los Angeles, CA, USA).

## Statistical analyses

All statistical analyses were performed using SPSS 16.0 (SPSS Inc.). Paired and unpaired 2-tailed Students' t-tests were used along with ANOVA (followed by Duncans test in case of significance) and Pearson correlation coefficient as well as chi-square, when appropriate. Accuracy was evaluated with bias and limits of agreement (± 1.96 SD) determined from a Bland-Altman (B-A) analysis [17]. Intra-and interobserver variability was expressed as standard error of a single determination (Smethod) using the formula, first proposed by Dahlberg [120]:

$$Smethod = \sqrt{(\Sigma di\ 2/(2n))},$$

where di is the difference between the i:th paired measurement and n is the number of differences. Smethod was also expressed as % of over all means. Single measure intraclass correlation coefficient (ICC) was also used to express interobserver variability. ICC assesses rating reliability by comparing the variability of different ratings of the same subject with the total variation across all ratings and all subjects [121, 122]. ICC above 0.6 is considered good and excellent if >0.75 [123]. Kappa measure of agreement was used to compare the estimated LVEF categories of visual assessment (EF ≥ 55%, 45–54%, 30–44%, and < 30%) and corresponding categorial values categorized from AutoEF, Manual Simpson and MPI (paper III).

In paper IV receiver-operator-characteristics (ROC) curve analyses were performed using the statistical programme MedCalc® Version 6.10 (MedCalc Software, Mariakerke, Belgium). Composite = strain radial*(0.024) + displacement radial*(0.455) – displacement longitudinal*(0.198) was calculated using the significant variables obtained from discriminant analysis.

# RESULTS

## Detection of myocardial ischemia with pulsed Tissue Doppler (Paper I)

### Patient-based analysis

The 26 patients included in the first study were divided into three groups according to the results from the myocardial perfusion SPECT: four patients had a normal SPECT, 10 had fully-reversible exercise-induced perfusion defects compatible with ischemia and 12 had fixed defects compatible with scar. Ten of the patients with scar had additional signs of exercise induced ischemia. New wall motion abnormalities during dobutamine stress were seen only in patients with scar on SPECT.

Patients with scar had a lower peak systolic velocity at rest in the basal and middle segments than patients with ischemia ($P<0.05$) (Table 2). Otherwise, the differences at rest were small between the groups. Patients with a normal SPECT had a higher peak systolic velocity during dobutamine infusion in the basal segments, $18.9 \pm 4.1$ cm $s^{-1}$, than patients with ischemia, $12.2 \pm 3.8$ ($P<0.001$) and scar $8.8 \pm 3.0$ ($P<0.005$). The middle segments showed a similar response to dobutamine as the basal segments but the peak systolic velocities were lower.

### Territory-based analysis

To investigate the regional influence of myocardial infarction and ischemia on myocardial velocity, the peak systolic velocity at rest and at peak dose were compared according to the vascular supply. On myocardial scintigraphy the anterior wall, septum and apex were assumed to represent the territory of the left anterior descending artery, the lateral wall to represent the left circumflex artery and the posterior wall the right coronary artery. On tissue Doppler the myocardial velocity in the basal part of the septum was assumed to represent the left anterior descending artery, the velocity in the basal part of the lateral wall to represent the left circumflex artery and the posterior wall the right coronary artery.

Forty-one territories had a normal SPECT, 22 had exercise-induced perfusion defects compatible with ischemia and 15 had resting and exercise defects compatible with scar with or without ischemia (Table 3). Territories with scar on SPECT had a lower peak systolic velocity at rest and at peak dose dobutamine in the basal segments than territories with a normal SPECT ($P<0.05$). However, the difference in peak systolic velocity at rest as well as at peak dose dobutamine

was less apparent between territories than between patients with normal and abnormal SPECT.

**Table 2.** Patient-based analysis.

Rest, peak stress and increase in peak systolic velocities (Vs) in patients with normal, ischemic, and scar SPECT results.

| | | **Normal (n=4)** | | **Ischemia (n = 10)** | | **Scar (n = 12)** |
|---|---|---|---|---|---|---|
| Vs rest (cm $s^{-1}$) | Basal | 7.9 ± 1.2 | Basal | 8.0 ± 2.1 | Basal | 6.5 ± 1.4$^{\dagger}$ |
| | Middle | 6.3 ± 0.9 | Middle | 5.8 ± 1.3 | Middle | 5.3 ± 0.9$^{\dagger}$ |
| Vs peak dobutamine | Basal | 18.9 ± 4.1 | Basal | 12. ±3.8*** | Basal | 8.8 ± 3.0** |
| (cm $s^{-1}$) | Middle | 14.4 ± 4.1 | Middle | 9.6 ± 3.1*** | Middle | 6.9 ± 3,3*$^{\dagger}$ |
| Increase (%) | Basal | 146 ± 74 | Basal | 54 ± 40*** | Basal | 34 ± 41* |
| | Middle | 139 ± 92 | Middle | 69 ± 49** | Middle | 34 ± 62 |

Mean ± SD
*p<0.05 vs. normal, **p<0.01 vs. normal, ***p<0.001 vs. normal, $^{\dagger}$p<0.05 vs. ischemia

**Table 3.** Territory-based analysis.

Rest, peak stress and increase in peak systolic velocities (Vs) in normal, ischemic, and scar territories on myocardial scintigraphy.

| | | **Normal (n=41)** | | **Ischemia (n = 22)** | | **Scar (n = 15)** |
|---|---|---|---|---|---|---|
| Vs rest (cm $s^{-1}$) | Basal | 7.6 ± 1.7 | Basal | 7.5 ± 2.4 | Basal | 6.3 ± 1.7* |
| | Middle | 5.9 ± 13 | Middle | 5.5 ± 1.4 | Middle | 5.2 ± 1.1 |
| Vs peak dobutamine | Basal | 12.6 ± 6.6 | Basal | 11.5 ± 3.6 | Basal | 9.3 ± 3.1* |
| (cm $s^{-1}$) | Middle | 9.7 ± 5.9 | Middle | 8.8 ± 3.0 | Middle | 7.9 ± 4.7 |
| Increase (%) | Basal | 65 ± 110 | Basal | 57 ± 39 | Basal | 50 ± 35 |
| | Middle | 73 ± 108 | Middle | 62 ± 45 | Middle | 61 ± 114 |

Mean ± SD
*p<0.05 vs. normal

In summary, we have shown that failure to achieve ≥13 cm $s^{-1}$ in peak systolic velocity (mean value of the basal segments in the three territories at peak dose dobutamine) in the patient-based analysis was the most accurate criterion for detection of significant CAD, i.e. ischemia and/or scar on SPECT. With this criterion, 18 of 22 patients with myocardial infarction and/or ischemia on SPECT and all four with a normal SPECT were correctly identified.
In the territory-based analysis, failure to achieve ≥12 cm $s^{-1}$ in peak systolic velocity at peak dose dobutamine in a basal segment was the most accurate criterion for detection of significant CAD. With this criterion, however, only 23 of 37 territories with myocardial infarction and/or ischemia on SPECT and 23 of 41 with a normal SPECT were correctly identified (sensitivity 62% and specificity 56%).

## Limitations

Some technical factors could have contributed to the low territorial agreement between tissue Doppler and SPECT. 2D echo depicts wall motion while scintigraphy visualizes tissue perfusion and therefore reflects an earlier step in the ischemic cascade. In the apical view, shortening velocities of the longitudinal fibers are measured and that velocity could be affected by tethering of the adjacent segments. There will also be an underestimation of the true myocardial velocity if the ultrasound beam is not parallel to the motion of the myocardium. The anatomic variations of the vascular territories were disregarded, e.g. the impact of RCA flow on the basal septal segment contraction when assigning the entire septum to the effects of flow in the LAD. No velocities were recorded in the anterior wall due to technical problems. Other limitations could be the use of different stressors with tissue Doppler and SPECT and also that the achieved stress-levels could have been inadequate. The effect of dobutamine at low doses is mainly inotropic and induces an increase in contractility in viable myocardium. New wall motion abnormalities were seen only in six patients.

## Diagnostic ability of TTDE in detecting significant stenosis in the LAD (Paper II)

TTDE without contrast visualized a distal segment of the LAD in 52 of the 69 patients and CFVR could be calculated in 48 patients (success rate 70%). No significant differences were found regarding age, gender, BMI, systolic blood pressure, known CAD (previous AMI, PCI and/or CABG), normal/abnormal myocardial SPECT between the group where CFVR was successfully calculated and the group where CFVR was not obtained.

The outcome in groups where CFVR was successfully calculated is summarized in table 4. TTDE identified coronary artery disease, defined from MPI as reversible ischemia and/or permanent defect, with a sensitivity of 60% and a specificity of 79%. The positive predictive value was calculated to 43% and the negative predictive value to 88%. Due to few patients with abnormal SPECT, the pre-test-probability was only 21%. The mean coefficient of variation for the calculation of CFVR, obtained by one operator (intraobserver variability), was 3.9%. Figure 9 shows the spread in individual CFVR values for patients with normal or abnormal MPI. There was no significant difference between the mean CFVR value for patients with normal MPI and for abnormal MPI (2.51 and 2.22 respectively, $p = 0.36$). The four patients shown in figure 9, having abnormal SPECT but CFVR >2 had spectral Doppler signals of good quality. Two of these patients had perfusion defects in territories of the right coronary artery (RCA) but not the LAD where CFVR was measured. In the third patient, the Doppler signal drifted into a stent in the LAD during stress thus giving a higher stress velocity and therefore a falsely high CFVR. The fourth patient had a stenosis in the anastomosis between the left internal mammary artery (LIMA) and the LAD causing an overestimation of CFVR. The eight patients with normal SPECT but reduced CFVR had all risk factors for endothelial dysfunction.

**Table 4.** Comparison between CFVR and MPI.

CFVR and result of MPI where CFVR was successfully calculated

| CFVR/MPI | Normal MPI | Abnormal MPI | Total |
|---|---|---|---|
| CFVR ≤2 | 8 | 6 | 14 |
| CFVR >2 | 30 | 4 | 34 |
| Total | 38 | 10 | 48 |

p=0.043, Chi square

MPI=myocardial perfusion imaging, CFVR=coronary flow velocity imaging

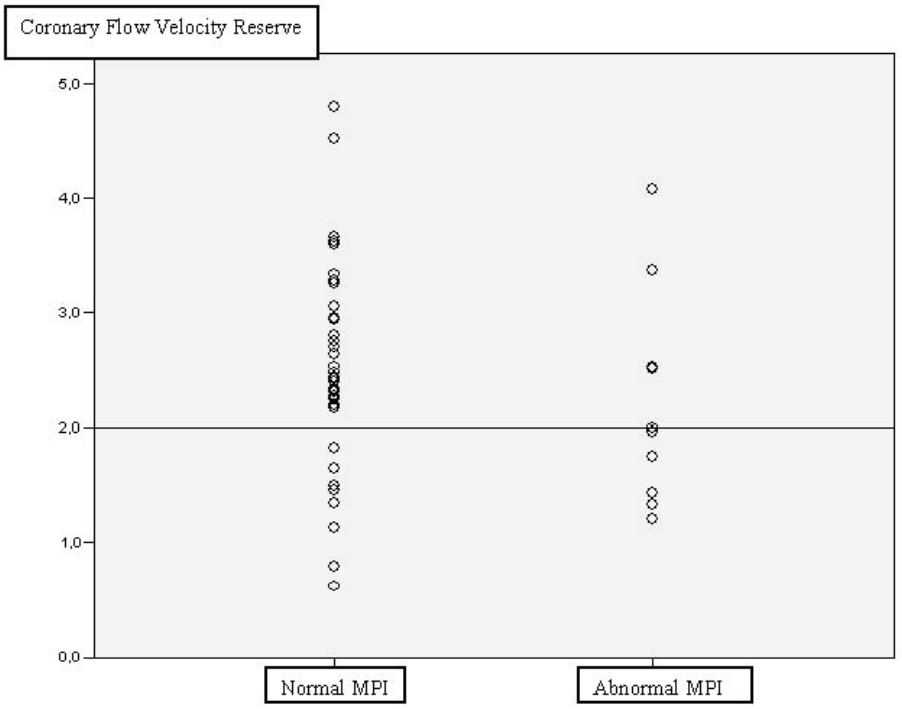


**Figure 9. Individual results of CFVR plotted against result of MPI.**
Heavy line indicates the limit for CFVR at 2.

## Limitations

The success rate was 70%, partly due to difficult scanning conditions in overweight patients and partly due to the discomfort induced by adenosine itself. We chose adenosine because of our familiarity with its properties. However, the hyperpnoea associated with the vasodilating effect of adenosine caused such discomfort that calculation of CFVR was impossible in some patients. We have also refrained from using external ultrasound contrast due to signal scattering in colour as well as in spectral Doppler recordings. Recent publications have shown that the use of ultrasound contrast improves the measurement of coronary flow velocity [66].

## Quantification of ejection fraction with a new semi-automatic diagnostic tool (Paper III)

Echocardiographic imaging was performed in 60 patients. No patient was excluded because of inferior image quality but one patient had to be excluded due to problems storing the images. The time required for analysis differed significantly between all the methods (p from < 0.001 to 0.015). Visual assessment and uncorrected AutoEF were the fastest (33 ± 14 s and 79 ± 5 s respectively) and corrected AutoEF and manual Simpson required the longest time (159 ± 46 s and 177 ± 66 s respectively).

There was a good agreement between the ejection fractions determined with the echocardiographic methods, Table 5. Manual Simpson gave significantly lower EF values than the other methods (p = 0.001–0.028), but no differences were seen between the other methods. Regardless of image quality, there were no differences between AutoEF (corrected and uncorrected) and manual Simpson. Ejection fraction from MPI was 52 ± 12%. MPI values > 65% were approximated to 65% (four patients) because of the partial volume effect [124]. Left ventricular volumes, normalized to body surface area, were largest for MPI, smallest for corrected and uncorrected AutoEF and intermediate for manual Simpson. Correlation analysis between corrected AutoEF, uncorrected AutoEF and manual Simpson (expert group) versus MPI showed coefficients of r = 0.77, 0.67 and 0.80, respectively, and limits of agreement 14.0%, 16.9% and 13.4% (LVEF units), respectively. The corresponding correlation coefficients were for the novices r = 0.73 and r = 0.68 for corrected AutoEF and manual Simpson, respectively (limits of agreement 15.2% and 16.3% LVEF units).
The estimated categories of LVEF by visual assessment compared to corresponding categorical values calculated for AutoEF, manual Simpson and MPI showed a moderate agreement: kappa measures of agreement were calculated to 0.47, 0.44, and 0.52, respectively for the expert readers. The corresponding value for AutoEF and manual Simpson was 0.53.

### Intra- and interobserver variability

For uncorrected AutoEF, the reproducibility was 100%. The intraobserver variability (Smethod by Dahlberg) for corrected AutoEF was for the expert readers 2.2 LVEF percentage points (4.7%) and for the novices 2.9 (6.4%). Corresponding values for manual Simpson were somewhat higher, for experienced readers, 3.5 LVEF percentage points (7.7%) and for novices 6.2 (14.6%). The difference in intraobserver variability between corrected AutoEF and manual Simpson was significant for both the experts (p = 0.004) and the novices (p = 0.008). As expected, experienced readers had significantly lower variability (p < 0.001).

The interobserver variability for the echocardiographic methods was analyzed both with the Smethod and the intraclass correlation coefficient (ICC). Highest ICC was found for corrected AutoEF (0.88 for experienced readers and 0.81 for novices) with corresponding values of Smethod of 3.5 (6.7%) and 4.4 (8.5%), respectively. ICC was lower for manual Simpson, especially novices (corresponding values 0.74 and 0.21) with values of Smethod 6.0 (11.6%) and 12.4 (25.7%), respectively, which demonstrates the low interrater agreement for the novices.

## Limitations

Most patients in this study had a normal or slightly reduced LVEF (44 of the 59 patients had LVEF > 45%). However, also in this patient category, it is important to determine small changes in LVEF considering the use of echo for monitoring potentially cardiotoxic drugs. LVEF and volumes determined with MPI are mean values over 20 minutes whereas EF and volumes from echocardiography are calculated from one beat. ECG-gated SPECT using 8 time frames has been shown to underestimate LVEF because of low frame rate and has also shown a tendency to overestimate high normal LVEF values due to partial volume effects in small hearts. In this study, only the supernormal LVEFs were corrected [19, 27]. MPI was used as reference to show that our volumes and calculated ejection fractions were plausible and was chosen because the patients in our study were referred for MPI which, as a by-product, gave us the ejection fraction measurement. MRI, being a gold standard for volume determination, was not possible to perform in the present setting in these patients. At the time of the study we did not have access to 3D echo. Even if many echo labs nowadays buy 3D capability, 2D-based methods will prevail in a medium term perspective due to the large installed base of contemporary ultrasound equipment. A larger number of novice readers would have been valuable, but was not available at the participating echo labs.

**Table 5.** Group results for the transthoracic echocardiographic and MPI variables

| | **Corrected AutoEF N = 59** (5 readers) | **Uncorrected AutoEF N = 59** (1 reader) | **Manual Simpson N = 59** (5 readers) | **MPI N = 59** (1 reader) |
|---|---|---|---|---|
| **LVEF (%)** | 53 ± 10 | 54 ± 10 | 51 ± 11 | 52 ± 12 |
| **EDV/BSA (mL/cm2)** | 53 ± 18 | 51 ± 16 | 56 ± 20 | 67 ± 26 |
| **ESV/BSA (mL/cm2)** | 26 ± 14 | 24 ± 13 | 28 ± 15 | 35 ± 23 |
| **Time for analysis (s)** | 174 ± 43 | 79 ± 5 | 190 ± 64 | |
| **Range (s)** | 96 - 417 | 68 - 90 | 100 - 615 | |

Mean ± SD
BSA = body surface area, EDV = End-diastolic volumes, ESV = end-systolic volumes, LVEF = left ventricular ejection fraction, MPI = myocardial perfusion imaging.

## Non-invasive detection of infarcted segments with high transmurality (Paper IV)

In the group of patients with scar (n=17), scar size was on average 31±12ml or 17±8% of the left ventricular myocardium. Twelve of the 17 patients had a scar percentage exceeding 12% which is considered prognostically unfavorable [125]. Left ventricular end-diastolic volume and end-systolic volume were significantly larger and LVEF lower in the group with scar compared with the group without scar.

In the scar group, transmurality was 52±39% in the segments belonging to LAD and 4±18% in the remote segments belonging to LCX or RCA. In one of the patients, the segment with >75% scar was located only in the apical cap. Eleven out of 119 remote segments showed small scar areas probably due to slight imperfections in the segmentation or due to the vascular supply being different from the standard segment model. Significant gadolinium uptake was not seen in the non-scar group.

### Functional measures

Results of the functional measures for the segments perfused by the LAD in the scar group compared with the corresponding segments in the non-scar group, stratified for degree of transmurality, are reported in Figure 10. In summary, for segments with a transmurality 51-75%, as well as for segments with a transmurality >75, significant differences were seen between scar and non-scar for all radial measures and for longitudinal strain. Longitudinal velocity and displacement showed lesser differences, probably due to difficulties in longitudinal tracking by the software. Receiver-operator-characteristics curves (ROC) were constructed for all measurements (Figure 11). They were primarily used to distinguish segments with scar transmurality >50% as well as >75% vs. nontransmural scar. Area-under-curves (AUC) for all measures vs. >50% transmurality are shown in table 6, where also sensitivity and specificity for different cut-off levels are given. Best AUC was for radial strain, where a cut-off value of <38.8% detected a segment with scar transmurality >50% within the LAD distribution with 80% sensitivity and 86% specificity. The composite measure of radial strain, radial and longitudinal displacement displayed only a marginal improvement in the AUC value. Global functional measurements (mean of 18 segments per patient) compared with MR-determined LVEF are shown in Figure 12. Best correlation was seen between the radial measures and LVEF in addition to longitudinal strain and LVEF.

### Intra- and interobserver variability

Intraobserver variability was estimated by two investigators from three repeated tracings on 5 patients in the scar and 5 in the non-scar groups. The mean of these three measurements was used for the calculation of interobserver variability according to Dahlberg. As a percentage of the mean, intraobserver variability was for radial measures 16-14-26% for displacement-velocity-strain and for the corresponding interobserver measurements 13-12-18%.

### Limitations

Feature tracking is a new approach for assessing myocardial motion. Some assumptions governing the function of the software are published as white papers by the developer, but most remain company secrets.

Strain has been shown to be sensitive to effects of afterload as well as ventricular size, being less in larger ventricles [126]. This might explain some of the findings in this study, where radial strain was significantly lower in the remote segments of the larger scarred ventricles compared to non-scarred ventricles. However, these differences were small. Blood pressure, which could have influenced the functional measures [127], was not recorded at the MRI examination.

In our study we investigated a limited group of patients with myocardial scar in the perfusion area of the LAD. A larger population ought to be investigated to confirm our findings, also including myocardial scars in the perfusion areas of RCA and LCX.

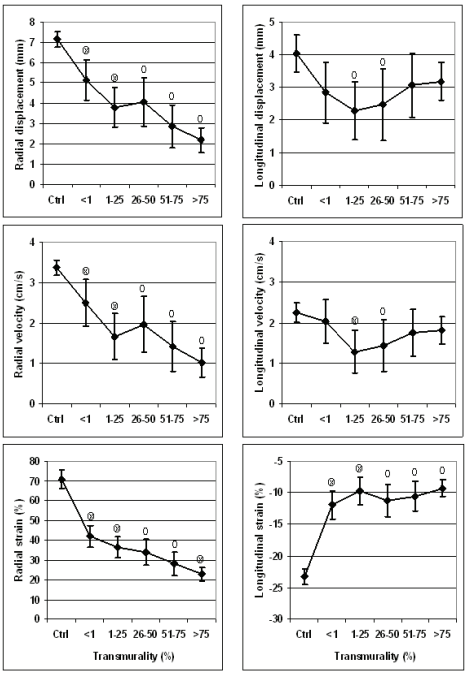


**Figure 10. Functional measures vs. transmurality, all patients (Ctrl = non-scar)**

o=denotes statistically significant difference ($p<0.05$) compared to controls (Ctrl)
x=denotes statistically significant difference ($p<0.05$) compared to nearest left value

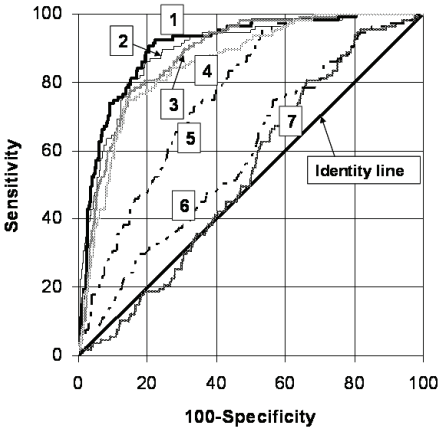


**Figure 11. ROC curves for the functional measures vs. >50% transmurality**

The composite of the radial measures strain-displacement-velocity shows only marginally larger AUC than radial strain alone. 1=Composite, 2=Radial strain, 3=Radial displacement, 4=Radial velocity, 5=Longitudinal strain, 6=Longitudinal velocity, 7=Longitudinal displacement

**Table 6. Areas under the receiver operator characteristic (ROC) curves (AUC) shown in Figure 9.**
The parameters are ranked after AUC. Sensitivities (sens) and specificities (spec) are in %.

| | Composite | Radial strain | Radial displacement | Radial velocity | Longitudinal strain | Longitudinal velocity | Longitudinal displacement |
|---|---|---|---|---|---|---|---|
| **ROC area** | 0.905 | 0.892 | 0.879 | 0.855 | 0.764 | 0.588 | 0.535 |
| **95% conf. int.** | 0.877-0.929 | 0.863-0.917 | 0.848-0.906 | 0.822-0.883 | 0.726-0.799 | 0.545-0.630 | 0.491-0.578 |
| **Cut off value*** | 2.52 | 38.8 | 3.97 | 1.82 | -18.5 | 2.49 | 4.99 |
| **Sens/Spec** | 78 / 93 | 80 / 86 | 85 / 78 | 86 / 75 | 47 / 95 | 44 / 75 | 34 / 80 |
| **Cut off value*** | >2.4 | >38.9 | >4.47 | >2.1 | <-9.6 | >1.1 | >1.29 |
| **Sens at Spec=80%** | 90 | 86 | 80 | 78 | 48 | 31 | 19 |

* Chosen cut off value corresponding to sensitivity and specificity in the row below

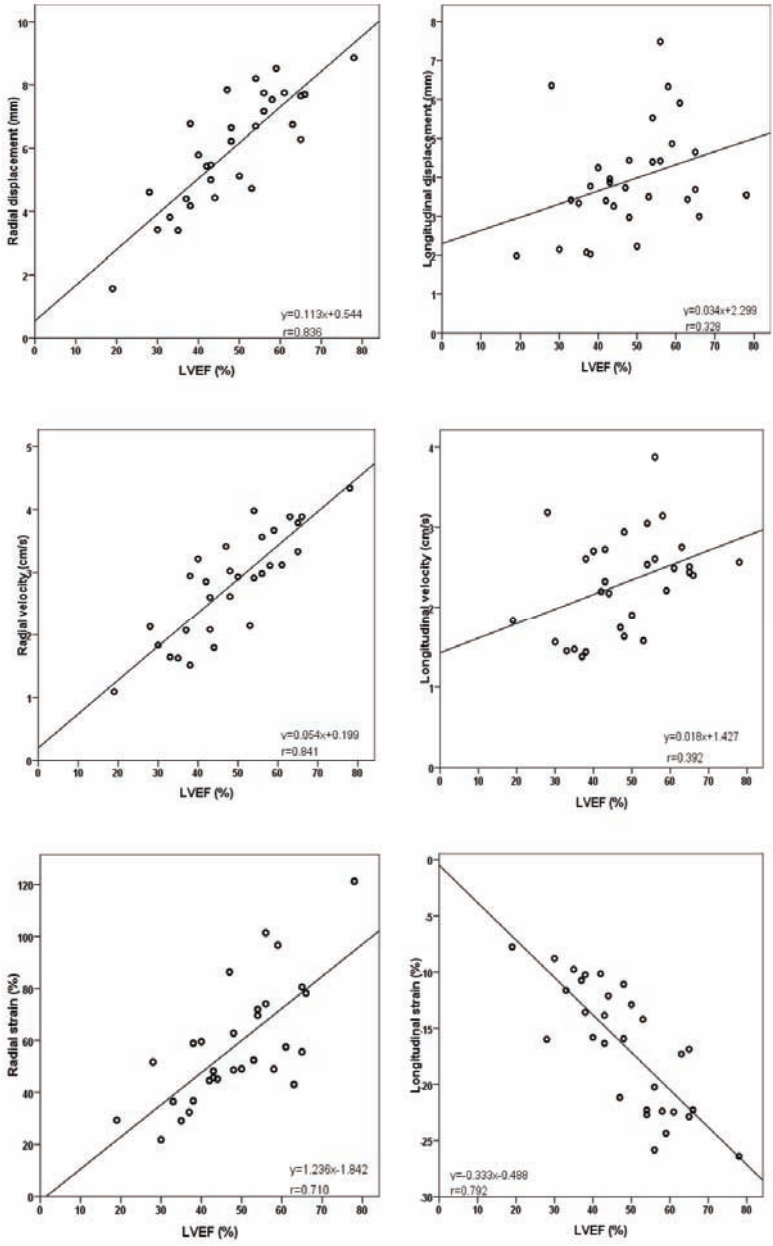


**Figure 12. Correlations between global functional measurements and MR determined LVEF**

# DISCUSSION

This thesis analyses several aspects of the cardiac response to the induction of myocardial ischemia. Generally, the progression from early to late changes has been referred to as "the ischemic cascade". It starts with subtle metabolic changes after only a few seconds of hypoperfusion, followed by diastolic filling abnormalities, systolic contraction delay, ischemic ST-deviation on the surface ECG and finally chest pain. These physiologic changes may all be investigated using different noninvasive techniques. In this discussion, the findings in the four papers will follow the path of the ischemic cascade.

## Transthoracic coronary Doppler detection of coronary vasomotion (Paper II)

In Paper II, the vasodilator reserve of the LAD was studied during adenosine infusion. Based on our findings, we suggest that CFVR >2 in the LAD will exclude significant coronary artery disease in a clinical setting but a low CFVR is more difficult to interpret since multiple cardiovascular and metabolic risk factors as well as epicardial vessel disease or microvascular dysfunction might be responsible.

Our study population contained patients with previous revascularization, hypertension, cardiomyopathies and diabetes mellitus. These conditions are associated with reduced endothelial function that might obscure the detection of coronary artery disease [128]. In addition, patients with LBBB/pacemaker/non-sinus rhythm and previous valve procedures were also included, which may explain the low sensitivity, 60%. Most previous validation studies of TTDE have not had this approach to patient selection [129-131]. The low pre-test-probability in our study (21% according to MPI) also influenced the sensitivity of transthoracic coronary Doppler. Adenosine, being a strong dilator of the coronary microcirculation, is considered to have little effect on the epicardial arteries [87], but as discussed earlier, Kiviniemi et al have shown that the epicardial coronary arteries increase in diameter up to 31% during adenosine infusion [89]. The increase in volume flow can therefore be underestimated and thereby the increase in coronary flow reserve. Changes in vasoactive medication were not undertaken according to our clinical routine for MPI studies. However, beta-blockers have been shown to increase CFVR while vasodilators have caused an underestimation of CFVR by reducing the maximal vasodilator response to adenosine [86].

In our opinion, TTDE is an attractive non-invasive method to evaluate chest pain without the use of isotope, but the diagnostic power is strongly dependent on the population investigated and the skill of the operator. In our study the success rate was 70%, which is at the same level as other investigators have achieved, without the use of external ultrasound contrast [66]. Recent publications have shown that the use of ultrasound contrast markedly improves the measurement of coronary flow velocity [66, 132, 133]. We limited TTDE scanning to the LAD and the result was compared with MPI in the LAD territory. However, other authors have shown the applicability of scanning all three coronary vessels [134].

### Future implications

TTDE is an interesting new tool in the diagnostic array of cardiovascular disease. The main strength is its (semi) non-invasiveness, freedom from radiation, availability and low cost. It is also easily repeatable and therefore well suited for follow-up after coronary interventions or for evaluating endothelial function over time following medical treatment. Different medical interventions can be evaluated in a physiological way. PET, being the golden standard for evaluation of CFR, is not suited for repeated studies due to radiation concerns and cost. Using adenosine as a vasodilatator enables very short study times. Maximal vasodilatation is attained after approximately 1-2 minutes and the very short half-life is in the range of 10 sec. Better ultrasound hardware, e.g. more channels, increased color Doppler sensitivity and better focused ultrasound probes could further improve future results.

## Use of tissue Doppler for the detection of ischemic wall motion (Paper I)

Diastolic filling abnormalities, generally believed to be the second step in the ischemic cascade, were not evaluated in this functional assessment of dobutamine stress, which focused on the next step, systolic contraction. The longitudinal shortening of the heart is a vital aspect of global systolic function, in addition to the radial thickening of the myocardial wall. A reduced longitudinal velocity and displacement may be early signs of ischemia affecting the longitudinal fibres of the ventricular wall. This contractile dysfunction may be difficult to perceive with the human eye.

Due to its absence of radiation, availability and relatively low cost, dobutamine stress echocardiography is an attractive method to induce and detect wall motion abnormalities secondary to myocardial ischemia. The investigator looks for a reduction of the endocardial excursion (the inward motion of the endocardium) induced by regional ischemia in real-time, which is a unique feature of echocar-

diography. However, a good diagnostic precision requires considerable experience (long learning curve) and even for very experienced readers the interpretation can vary due to their subjectivity (visual interpretation). The use of intravenous contrast might improve the detection of subtle wall motion abnormalities during stress due to better delineation of the endocardial border. But still, objective means are needed to aid the less experienced reader of echo images.
Tissue Doppler quantifies the longitudinal shortening in myocardial segments at rest and at stress. We showed that failure to achieve ±13 cm $s^{-1}$ in peak systolic velocity during dobutamine stress in the patient-based analysis was the best cut-off for the detection of CAD in patients. The findings in our study agreed well with similar studies reported at that time [135] who also showed the additive effect of pulsed tissue Doppler to the visual interpretation of stress echocardiography. Some studies emphasized that the cut-off-values for the peak systolic velocities had to be adjusted for heart rate, age and gender [136].

Future implications

Due to the very high temporal resolution of the method, changes in short time-phases can be analyzed and followed, changes not always visible to the eye. In our study, we analyzed only the peak systolic velocities in different segments, but reversible myocardial ischemia affects diastolic function earlier than systolic function. Therefore, analysis of the diastolic components, as well as the isovolumetric phases, can be of interest. Pulsed tissue Doppler allows us to gain a better understanding of the velocities and temporal phases during the cardiac cycle, not only in ischemic heart disease but also in cardiomyopathies, right ventricular disease and in understanding and diagnosis of left ventricular dyssynchrony.

Doppler tissue imaging (DTI) allows semi-quantification of myocardial motion and also postprocessing off line from multiple sites. The acquisition requires a few seconds without compromising the stress-study, though the post-processing and analysis off-line might be more time consuming. DTI allows differences in velocities from the endocardium to the epicardium to be evaluated, as well as quantifying the motion within a myocardial segment and the diastolic parameters. The development of myocardial strain rate and strain imaging may further improve the quantification of regional ischemia. Strain rate is the difference in tissue velocity per unit length, or rate by which deformation occurs. Integrating this parameter reveals deformation or strain, a measure of the compression of myocardium during systole [137].

| | |
|---|---|
| Strain rate = (V2-V1)/d, | where V1 and V2 are velocities of shortening at two points separated by distance d |
| Strain = (L1-L2)/L1, | where L1 is the distance between two points at end-diastole and L2 is the distance between the same points at end-systole |

Among the obstacles limiting the clinicians´ understanding are the differences in terminology and the variety of software solutions produced by the manufacturers. It is therefore difficult to compare and evaluate studies using different equipment. Strain by speckle tracking has been validated experimentally by ultrasonomicrometry [138, 139]. The reflected ultrasound of the myocardium is inhomogeneous, giving rise to an irregular echo-pattern, speckles. The speckles follow the motion of the myocardium and are unique in each segment and therefore possible to follow throughout the cardiac cycle. Velocities, strain and strain rate can be assessed independently from the angle of insonation. Development of automatic evaluation of speckle-tracking should make the method even more attractive and some studies have already shown the predictive value of global strain measures. For example, Bjork Ingul et al have shown that mortality can be predicted by segmental analysis of strain rate during dobutamine stress [140]. Further use of quantitative methods should enable a wider use of stress echo for dynamic assessment of coronary disease.

## How accurate is the measurement of systolic LV function by echo? (Paper III)

Left ventricular end-diastolic volume, ejection fraction (LVEF) and wall thickness are strong predictors for survival in coronary heart disease but also in most types of other cardiac diseases. These measurements have important implications for therapy. The optimal timing for supportive surgery for heart failure such as ventricular restraint, ventricular restoration and left ventricular assist device surgery as well as valve surgery all rely upon measures of volume and LVEF, not to mention decisions on resynchronisation therapy, implantation of cardiac defibrillators and monitoring of anti-neoplastic drug treatment [141-143]. The measurement of cardiac volumes and ejection fraction should be accurate and reproducible, easy to use, affordable, non-invasive and without radiation exposure to the patient. Two-dimensional echocardiography can fulfill many of the requirements on the clinician's wish list and has captured a central role in the clinical setting. It is widely used but demanding on the operator and sensitive to poor acoustic windows. Most frequently, quantification of LV function is performed by visual estimation. Reports have claimed high accuracy in comparison with more objective methods, at least for trained observers [144, 145]. The echocardiographic quantification method recommended by the European Society of Cardiology [118] is the biplane method of discs (modified Simpson's rule). The method is time-consuming, requires optimal visualization of the endocardial border and substantial expertise.

In our study, we show for the first time a reduced variability in the measurement of ejection fraction when experienced and novice readers use biplane AutoEF. Due to AutoEF, intra- and interobserver variability was reduced compared with manual biplane planimetry, especially for novice readers (Figure 13). The addition of manual corrections to AutoEF produced somewhat better estimates of volumes but not of LVEF. Without manual correction, the application of AutoEF on the scanner took on average 79 s.

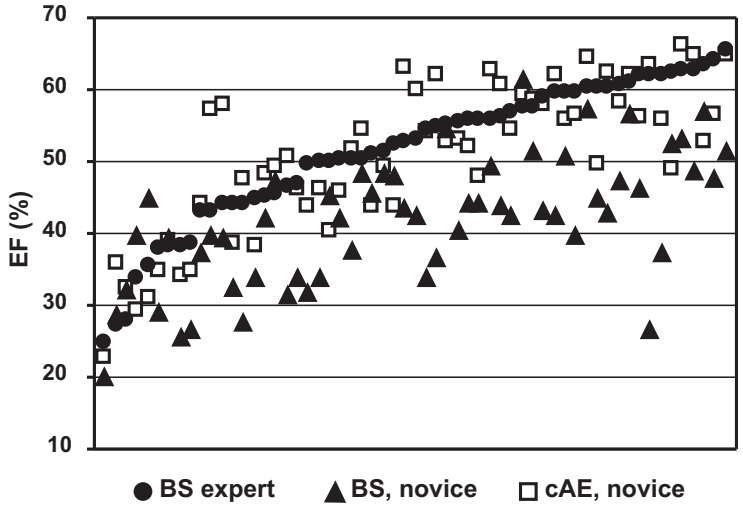


**Figure 13. Effect of computer-assisted measurements on novice performance.**
Plot of left ventricular ejection fraction (LVEF%), ranked after increasing values of the expert manual Simpson (filled circles). Values in line above and below BS expert belong to the same patient and show corresponding values for novice manual Simpson (filled triangle) and novice corrected AutoEF (empty square). The smallest deviation from expert manual Simpson is seen for novice corrected AutoEF. BS = manual Simpson, MPI = myocardial perfusion imaging, LVEF = left ventricular ejection fraction

Computer software is often protected by commercial intellectual property rights that make an open comparison difficult. According to personal communications with developers, the reference population was studied with the apical 4-chamber view in 528 clips of which 67% had EF<45%. The number of apical 2-chamber views was less, 428 clips, where 63% had <45% EF. Thus, the validation of the method was performed mostly on images from patients with a reduced ejection fraction, while such patients were a minority in our study.

In contrast to previous studies, we did not exclude patients on the basis of image quality. Those with poor image quality showed a similar agreement compared to MPI as those with good image quality. To avoid bias in studies like this, it is necessary to properly blind the image readers, as well as use a reference method in all patients. Both conditions were successfully applied.
In a comparison between methods, precision ("accuracy") is as important as a low random variation in measurements. Accuracy is dependent on the reference method used. A better agreement is expected if the reference method uses identical images, as in this study where AutoEF was compared with manual planimetry on echocardiographic images. Both echo-based methods use one heart beat for the calculation of LVEF, while SPECT uses information selected during an acquisition that takes on average 20 minutes.

Is visual assessment a viable alternative to AutoEF for the determination of LVEF? Some studies [144] have reported enthusiastic positive experience of using eye-balling, even at a level of determining single percentage points of LVEF. McGowan, however, in a recent meta-analysis expressed a more guarded attitude [146]. Methods like AutoEF are of great value, especially for the novices. In our hands, this method seems to be able to reduce variation in the assessment of LVEF in clinical patients.

### Future implications

Echocardiography plays a central role in cardiovascular diagnostics. Due to its availability, low cost, non-invasiveness and freedom from radiation, it is often the first investigation made in a patient with suspected heart disease. The reasons for referral are broad and the numbers of investigations are increasing worldwide. Due to the rather low costs of purchase – a very simple handheld echo-machine can cost as little as 10 000 USD, more powerful scanners maybe 30-60 000 USD, also primary care physicians have interest in investigating and screening their own patients. In this setting, (semi-) automated tools to assess ejection fraction with optimal accuracy and reproducibility without advanced or time-consuming post-processing are needed. Evaluation of medical or surgical treatment might be repeatedly performed, with less dependency on the experience of the investigator or on the administration of intravenous contrast. Real time 3-D echocardiography is a promising future approach [147], but optimal signal-to-noise ratio and delineation of the endocardial border are still crucial for producing accurate values of ejection fraction.

## Can contrast enhanced MRI be replaced by strain analysis cine MRI? (Paper IV)

As a late step in the ischemic cascade, reduction in wall motion is the hallmark of myocardial damage and the resulting reduction in left ventricular ejection fraction has been shown to be an important prognostic factor. The transmurality of the myocardial scar is another strong prognostic parameter best determined with late gadolinium enhancement imaging [102, 103, 106]. In our study, we show for the first time the ability to differentiate segments with various transmurality without the need for the administration of gadolinium-based contrast. We have shown that the feature-tracking software is able to track left ventricular wall motion with good precision, as shown by low intra- and interobserver variability. Scarred myocardial segments perfused by the LAD can be differentiated from the corresponding non-scar segments using any of the three radial parameters, but most of the information is contained in the measurement of radial strain. We also show that a cut-off value of 38.8% in radial strain identifies segments with >50% infarct transmurality. Longitudinal motion seems more difficult to track, even if segments with and without scar may be differentiated with the aid of longitudinal strain, in line with previous reports using an earlier version of the software applied to echocardiographic images [148]. The global average of the radial measures correlated well with LVEF (View Forum) indicating that these measurements have a validity that can be corroborated by more frequently used parameters.

### Future implications

The feature tracking software is an attractive post processing tool, yet only in the beginning of comprehensive understanding and still to be fully evaluated. The possibility to objectively investigate and understand regional and general myocardial motion in a variety of cardiac diseases is an exciting challenge. The software also provides information about time phases, as time to peak and phase, which we are currently exploring. It might give additional information about the motion of infarcted segments, but might also be of great interest in selecting patients with heart failure and dyssynchronic motion that could benefit from resynchronization therapy. Due to the fact that the analysis is made on cine MR images without the need of additional sequences (i.e. tagging) and that intravenous injection of gadolinium is avoided, the examination time in the MR camera can be shortened, therefore limiting costs and avoiding potentially toxic agents.

In summary, the ischemic cascade guides us along the path of reversible and irreversible left ventricular damage. Quantitation is the basis for correct selection of patient treatments. Echocardiography, MRI and nuclear techniques are all useful in this work-up of patients, and should be used according to their strengths and weaknesses.

# CONCLUSIONS

Based on four different studies involving in total 185 patients, the following conclusions can be drawn:

*…on myocardial ischemia*

- A reduced longitudinal velocity and displacement are early signs of ischemia affecting the longitudinal fibers of the ventricular wall. In our hands, pulsed tissue Doppler was successfully used for objective quantification of left ventricular longitudinal shortening and for differentiation between patients with normal, ischemic or necrotic myocardium according to single photon emission computed tomography results. However, we could not identify myocardial ischemia or scar in individual vascular territories.

- Transthoracic Doppler echocardiography is an attractive non-invasive method for the evaluation of chest pain without the use of isotope. We suggest that in a clinical setting, coronary flow velocity reserve >2 in the left anterior descending artery will exclude significant coronary artery disease. A low coronary flow velocity reserve is more difficult to interpret since multiple cardiovascular and metabolic risk factors as well as epicardial vessel disease or microvascular dysfunction might be responsible. This promising tool is well suited for follow-up after coronary interventions or for evaluating endothelial function over time following medical treatment.

*…on left ventricular function*

- A reduction in wall motion is the hallmark of myocardial damage and the resulting reduction in left ventricular ejection fraction is an important prognostic factor. We have shown that a computer software using learned pattern recognition and artificial intelligence (AutoEF) applied on biplane apical echocardiographic views reduces the variation in measurements compared with manual planimetry without increasing the time required. In our hands, this method reduces variation in the assessment of left ventricular ejection fraction in clinical patients.

- The transmurality of a myocardial scar, as observed with late gadolinium enhancement magnetic resonance imaging, is a strong prognostic parameter that can be determined with the feature tracking software Diogenes-MRI. Scar transmurality >50% within the LAD distribution can be determined already from an analysis of cine-MRI with 80% sensitivity and 86% specificity, without the need for the administration of gadolinium-based contrast.

# ACKNOWLEDGEMENTS

This thesis would never have been possible without the contribution, support and help from many people. I wish to express my appreciation to all of you and my special gratitude to:

**Jan Ohlsson**, associate professor and my supervisor for accepting the heavy burden of guiding and supporting me through this work. No one but you can make me feel the thrill in building an Access database and your aim to reach perfection is estimable. Your support has been invaluable.

**Eva Nylander**, professor and co-supervisor, for your interest and patience throughout these years. With your scientific knowledge and firm guidance you are my role model.

**Jan Engvall**, associate professor and co-author, for introducing me to the exciting and never ending world of science. Your enthusiasm is contagious, your optimism never ending and your endurance admirable. You have always been encouraging, seeing possibilities even in the most immature ideas and eagerly sharing your knowledge. This one is for you!

**Lars Brudin**, professor and co-author, for fruitful collaboration, always responding in a split second (even during Christmas holidays!) on our never ending statistical questions. You have given me an insight in how statistical analyses of data should be performed and organized. I am impressed!

**Peter Blomstrand**, **Jan-Erik Karlsson, Lena Lindström, Mårten Scheike**, **Eva Swahn, Kåge Säfström** and **Tim Tödt**, co-authors, and also **Robin Kardell, Dawid Kusiak** and **Monika Liehl**, for participation and contribution in the studies.

**Pearl Ohlsson**, for the excellent linguistic revision of the manuscripts in close association with her husband Jan Ohlsson. You´re a first-rate team!

**Peter Blomstrand**, head of the Department of Clinical Physiology, Ryhov County Hospital, for enabling me to focus on these studies.

All the staff at the Department of Clinical Physiology, especially **Magnus Franzén, Johan Homelius, Tina Landin, Magdalena Lemke** and **Lars Persson**, for your positive attitude and patience whenever a new study was initiated and your professional skills in performing some of the investigations.

My **colleagues** at the Department of Clinical Physiology for substituting for me when I was absent from the daily clinical work.

**Bo-Erik Malmvall**, professor and head of FUTURUM, the Academy for Healthcare, Jönköping County Council, for your support and always finding a way to solve a problem.

**Oskar Löfgren**, head of the Department of Radiology, Ryhov County Hospital, and his **staff** for good collaboration in cardiac MRI.

My **friends**, close and far away, for the encouragement and all the laughs, for finding time for an After-work-session or for a SPA-weekend, but also for lending me your ear when life is troublesome. I cherish your friendship.

My **Mother** and late **Father**, for giving me a solid start in life.

Last but absolutely not least, my fearless sons, **Martin** and **John**. I am so excited to follow and support you on your path in life. You make my life worth living!

The studies, upon which this thesis is based, were supported by grants from **FUTURUM**, the Academy for Healthcare, Jönköping County Council, **FORSS**, the Medical Research Council of Southeast Sweden, **CMIV**, the Centre for Medical Image Science and Visualization, Linköping University Hospital, the **Swedish Research Council** and the **Swedish Heart-Lung Foundation**.

# BIBLIOGRAPHY


1. *Nationella riktlinjer för hjärtsjukvård 2008*. ed. The National Board of Health and Wellfare 2008.
2. Emond, M., et al., *Long-term survival of medically treated patients in the Coronary Artery Surgery Study (CASS) Registry.* Circulation, 1994. **90**(6): p. 2645-57.
3. Muhlbaier, L.H., et al., *Observational comparison of event-free survival with medical and surgical therapy in patients with coronary artery disease. 20 years of follow-up.* Circulation, 1992. **86**(5 Suppl): p. II198-204.
4. Feigl, E.O., *Coronary physiology.* Physiol Rev, 1983. **63**(1): p. 1-205.
5. Gould, K.L. and K. Lipscomb, *Effects of coronary stenoses on coronary flow reserve and resistance.* Am J Cardiol, 1974. **34**(1): p. 48-55.
6. Gould, K.L., K. Lipscomb, and G.W. Hamilton, *Physiologic basis for assessing critical coronary stenosis. Instantaneous flow response and regional distribution during coronary hyperemia as measures of coronary flow reserve.* Am J Cardiol, 1974. **33**(1): p. 87-94.
7. Gould, K.L., R.L. Kirkeeide, and M. Buchi, *Coronary flow reserve as a physiologic measure of stenosis severity.* J Am Coll Cardiol, 1990. **15**(2): p. 459-74.
8. Kern, M.J., et al., *Physiological assessment of coronary artery disease in the cardiac catheterization laboratory: a scientific statement from the American Heart Association Committee on Diagnostic and Interventional Cardiac Catheterization, Council on Clinical Cardiology.* Circulation, 2006. **114**(12): p. 1321-41.
9. Hansson, G.K. and J. Nilsson, *Introduction: atherosclerosis as inflammation: a controversial concept becomes accepted.* J Intern Med, 2008. **263**(5): p. 462-3.
10. Sigwart, U., *Ischemic events during coronary artery balloon obstruction*, in *Silent myocardial ischemia*, W.R. Rutishauser, H. , Editor. 1984, Springer-Verlag: Berlin.
11. Reimer, K.A., et al., *The wavefront phenomenon of ischemic cell death. 1. Myocardial infarct size vs duration of coronary occlusion in dogs.* Circulation, 1977. **56**(5): p. 786-94.
12. Reimer, K.A. and R.B. Jennings, *The "wavefront phenomenon" of myocardial ischemic cell death. II. Transmural progression of necrosis within the framework of ischemic bed size (myocardium at risk) and collateral flow.* Lab Invest, 1979. **40**(6): p. 633-44.
13. Vargas, S.O., B.A. Sampson, and F.J. Schoen, *Pathologic detection of early myocardial infarction: a critical review of the evolution and usefulness of modern techniques.* Mod Pathol, 1999. **12**(6): p. 635-45.
14. MacCarthy, P.A., et al., *Prognosis in heart failure with preserved left ventricular systolic function: prospective cohort study.* BMJ, 2003. **327**(7406): p. 78-9.
15. Forrester, J.S., et al., *Functional significance of regional ischemic contraction abnormalities.* Circulation, 1976. **54**(1): p. 64-70.
16. White, H.D., et al., *Left ventricular end-systolic volume as the major determinant of survival after recovery from myocardial infarction.* Circulation, 1987. **76**(1): p. 44-51.
17. Braunwald, E. and J.D. Rutherford, *Reversible ischemic left ventricular dysfunction: evidence for the "hibernating myocardium".* J Am Coll Cardiol, 1986. **8**(6): p. 1467-70.
18. Elefteriades, J.A., et al., *Coronary artery bypass grafting in severe left ventricular dysfunction: excellent survival with improved ejection fraction and functional state.* J Am Coll Cardiol, 1993. **22**(5): p. 1411-7.
19. Rahimtoola, S.H., *The hibernating myocardium.* Am Heart J, 1989. **117**(1): p. 211-21.
20. Ross, J., Jr., *Myocardial perfusion-contraction matching. Implications for coronary heart disease and hibernation.* Circulation, 1991. **83**(3): p. 1076-83.

21. Canty, J.M., Jr. and J.A. Fallavollita, *Chronic hibernation and chronic stunning: a continuum.* J Nucl Cardiol, 2000. **7**(5): p. 509-27.
22. Braunwald, E. and R.A. Kloner, *The stunned myocardium: prolonged, postischemic ventricular dysfunction.* Circulation, 1982. **66**(6): p. 1146-9.
23. Heyndrickx, G.R., et al., *Depression of regional blood flow and wall thickening after brief coronary occlusions.* Am J Physiol, 1978. **234**(6): p. H653-9.
24. Kloner, R.A. and R.B. Jennings, *Consequences of brief ischemia: stunning, preconditioning, and their clinical implications: part 2.* Circulation, 2001. **104**(25): p. 3158-67.
25. Matsuzaki, M., et al., *Sustained regional dysfunction produced by prolonged coronary stenosis: gradual recovery after reperfusion.* Circulation, 1983. **68**(1): p. 170-82.
26. Rahimtoola, S.H., *A perspective on the three large multicenter randomized clinical trials of coronary bypass surgery for chronic stable angina.* Circulation, 1985. **72**(6 Pt 2): p. V123-35.
27. Di Carli, M.F., et al., *Long-term survival of patients with coronary artery disease and left ventricular dysfunction: implications for the role of myocardial viability assessment in management decisions.* J Thorac Cardiovasc Surg, 1998. **116**(6): p. 997-1004.
28. Bailar, J.C., 3rd, *The promise and problems of meta-analysis.* N Engl J Med, 1997. **337**(8): p. 559-61.
29. LeLorier, J., et al., *Discrepancies between meta-analyses and subsequent large randomized, controlled trials.* N Engl J Med, 1997. **337**(8): p. 536-42.
30. Allman, K.C., et al., *Myocardial viability testing and impact of revascularization on prognosis in patients with coronary artery disease and left ventricular dysfunction: a meta-analysis.* J Am Coll Cardiol, 2002. **39**(7): p. 1151-8.
31. Gill, C.J., L. Sabin, and C.H. Schmid, *Why clinicians are natural bayesians.* BMJ, 2005. **330**(7499): p. 1080-3.
32. Goodman, S.N., *Toward evidence-based medical statistics. 2: The Bayes factor.* Ann Intern Med, 1999. **130**(12): p. 1005-13.
33. Roelandt, J.R., *The 50th anniversary of echocardiography: are we at the dawn of a new era?* Eur J Echocardiogr, 2003. **4**(4): p. 233-6.
34. Monaghan, M.J., *Stress myocardial contrast echocardiography.* Heart, 2003. **89**(12): p. 1391-3.
35. Senior, R., et al., *Contrast echocardiography: evidence-based recommendations by European Association of Echocardiography.* Eur J Echocardiogr, 2009. **10**(2): p. 194-212.
36. Bhan, A., et al., *Real-time three-dimensional myocardial contrast echocardiography: is it clinically feasible?* Eur J Echocardiogr, 2008. **9**(6): p. 761-5.
37. Bom, N., C.T. Lancee, and F.C. Van Egmond, *An ultrasonic intracardiac scanner.* Ultrasonics, 1972. **10**(2): p. 72-6.
38. Cieszynski, T., *[Intracardiac method for the investigation of structure of the heart with the aid of ultrasonics.].* Arch Immunol Ther Exp (Warsz), 1960. **8**: p. 551-7.
39. Omoto, R., *Intracardiac scanning of the heart with the aid of ultrasonic intravenous probe.* Jpn Heart J, 1967. **8**(6): p. 569-81.
40. Detre, K.M., et al., *Observer agreement in evaluating coronary angiograms.* Circulation, 1975. **52**(6): p. 979-86.
41. Galbraith, J.E., M.L. Murphy, and N. de Soyza, *Coronary angiogram interpretation. Interobserver variability.* JAMA, 1978. **240**(19): p. 2053-6.
42. Zir, L.M., et al., *Interobserver variability in coronary angiography.* Circulation, 1976. **53**(4): p. 627-32.
43. Doucette, J.W., et al., *Validation of a Doppler guide wire for intravascular measurement of coronary artery flow velocity.* Circulation, 1992. **85**(5): p. 1899-911.
44. Tonino, P.A., et al., *Fractional flow reserve versus angiography for guiding percutaneous coronary intervention.* N Engl J Med, 2009. **360**(3): p. 213-24.
45. Bech, G.J., et al., *Fractional flow reserve to determine the appropriateness of angioplasty in moderate coronary stenosis: a randomized trial.* Circulation, 2001. **103**(24): p. 2928-34.

46. De Bruyne, B., et al., *Abnormal epicardial coronary resistance in patients with diffuse atherosclerosis but "Normal" coronary angiography.* Circulation, 2001. **104**(20): p. 2401-6.
47. De Bruyne, B., et al., *Fractional flow reserve in patients with prior myocardial infarction.* Circulation, 2001. **104**(2): p. 157-62.
48. Pijls, N.H., et al., *Measurement of fractional flow reserve to assess the functional severity of coronary-artery stenoses.* N Engl J Med, 1996. **334**(26): p. 1703-8.
49. Kuhle, W.G., et al., *Quantification of regional myocardial blood flow using 13N-ammonia and reoriented dynamic positron emission tomographic imaging.* Circulation, 1992. **86**(3): p. 1004-17.
50. Muzik, O., et al., *Validation of nitrogen-13-ammonia tracer kinetic model for quantification of myocardial blood flow using PET.* J Nucl Med, 1993. **34**(1): p. 83-91.
51. Miller, D.D., et al., *MRI detection of myocardial perfusion changes by gadolinium-DTPA infusion during dipyridamole hyperemia.* Magn Reson Med, 1989. **10**(2): p. 246-55.
52. Wilke, N., et al., *Contrast-enhanced first pass myocardial perfusion imaging: correlation between myocardial blood flow in dogs at rest and during hyperemia.* Magn Reson Med, 1993. **29**(4): p. 485-97.
53. Cullen, J.H., et al., *A myocardial perfusion reserve index in humans using first-pass contrast-enhanced magnetic resonance imaging.* J Am Coll Cardiol, 1999. **33**(5): p. 1386-94.
54. Larsson, H.B., et al., *Myocardial perfusion modeling using MRI.* Magn Reson Med, 1996. **35**(5): p. 716-26.
55. Ibrahim, T., et al., *Assessment of coronary flow reserve: comparison between contrast-enhanced magnetic resonance imaging and positron emission tomography.* J Am Coll Cardiol, 2002. **39**(5): p. 864-70.
56. Kurita, T., et al., *Regional myocardial perfusion reserve determined using myocardial perfusion magnetic resonance imaging showed a direct correlation with coronary flow velocity reserve by Doppler flow wire.* Eur Heart J, 2009. **30**(4): p. 444-52.
57. Schwitter, J., et al., *Magnetic resonance-based assessment of global coronary flow and flow reserve and its relation to left ventricular functional parameters: a comparison with positron emission tomography.* Circulation, 2000. **101**(23): p. 2696-702.
58. Caiati, C., et al., *New noninvasive method for coronary flow reserve assessment: contrast-enhanced transthoracic second harmonic echo Doppler.* Circulation, 1999. **99**(6): p. 771-8.
59. Caiati, C., et al., *Contrast-enhanced transthoracic second harmonic echo Doppler with adenosine: a noninvasive, rapid and effective method for coronary flow reserve assessment.* J Am Coll Cardiol, 1999. **34**(1): p. 122-30.
60. Crowley, J.J. and L.M. Shapiro, *Transthoracic echocardiographic measurement of coronary blood flow and reserve.* J Am Soc Echocardiogr, 1997. **10**(4): p. 337-43.
61. Hozumi, T., et al., *Noninvasive assessment of coronary flow velocity and coronary flow velocity reserve in the left anterior descending coronary artery by Doppler echocardiography: comparison with invasive technique.* J Am Coll Cardiol, 1998. **32**(5): p. 1251-9.
62. Saraste, M., et al., *Technical achievement: transthoracic Doppler echocardiography can be used to detect LAD restenosis after coronary angioplasty.* Clin Physiol, 2000. **20**(6): p. 428-33.
63. Auriti, A., et al., *Distal left circumflex coronary artery flow reserve recorded by transthoracic Doppler echocardiography: a comparison with Doppler-wire.* Cardiovasc Ultrasound, 2007. **5**: p. 22.
64. Voci, P., et al., *[Visualization of native internal mammary arteries and aorto-coronary graft by means of high resolution color Doppler ultrasonography].* Cardiologia, 1998. **43**(4): p. 403-6.

65. Voci, P., G. Testa, and G. Plaustro, *Imaging of the distal left anterior descending coronary artery by transthoracic color-Doppler echocardiography.* Am J Cardiol, 1998. **81**(12A): p. 74G-78G.
66. Okayama, H., et al., *Usefulness of an echo-contrast agent for assessment of coronary flow velocity and coronary flow velocity reserve in the left anterior descending coronary artery with transthoracic doppler scan echocardiography.* Am Heart J, 2002. **143**(4): p. 668-75.
67. Saraste, M., et al., *Transthoracic Doppler echocardiography as a noninvasive tool to assess coronary artery stenoses--a comparison with quantitative coronary angiography.* J Am Soc Echocardiogr, 2005. **18**(6): p. 679-85.
68. Saraste, M., et al., *Coronary flow reserve: measurement with transthoracic Doppler echocardiography is reproducible and comparable with positron emission tomography.* Clin Physiol, 2001. **21**(1): p. 114-22.
69. Lethen, H., et al., *Validation of noninvasive assessment of coronary flow velocity reserve in the right coronary artery. A comparison of transthoracic echocardiographic results with intracoronary Doppler flow wire measurements.* Eur Heart J, 2003. **24**(17): p. 1567-75.
70. Lethen, H., et al., *Comparison of transthoracic Doppler echocardiography to intracoronary Doppler guidewire measurements for assessment of coronary flow reserve in the left anterior descending artery for detection of restenosis after coronary angioplasty.* Am J Cardiol, 2003. **91**(4): p. 412-7.
71. Caiati, C., et al., *Validation of a new noninvasive method (contrast-enhanced transthoracic second harmonic echo Doppler) for the evaluation of coronary flow reserve: comparison with intracoronary Doppler flow wire.* J Am Coll Cardiol, 1999. **34**(4): p. 1193-200.
72. Heller, L.I., et al., *Intracoronary Doppler assessment of moderate coronary artery disease: comparison with 201Tl imaging and coronary angiography. FACTS Study Group.* Circulation, 1997. **96**(2): p. 484-90.
73. Serruys, P.W., et al., *Prognostic value of intracoronary flow velocity and diameter stenosis in assessing the short- and long-term outcomes of coronary balloon angioplasty: the DEBATE Study (Doppler Endpoints Balloon Angioplasty Trial Europe).* Circulation, 1997. **96**(10): p. 3369-77.
74. Okayama, H., et al., *Assessment of intermediate stenosis in the left anterior descending coronary artery with contrast-enhanced transthoracic Doppler echocardiography.* Coron Artery Dis, 2003. **14**(3): p. 247-54.
75. Pizzuto, F., et al., *Noninvasive coronary flow reserve assessed by transthoracic coronary Doppler ultrasound in patients with left anterior descending coronary artery stents.* Am J Cardiol, 2003. **91**(5): p. 522-6.
76. Hozumi, T., et al., *Coronary flow velocity analysis during short term follow up after coronary reperfusion: use of transthoracic Doppler echocardiography to predict regional wall motion recovery in patients with acute myocardial infarction.* Heart, 2003. **89**(10): p. 1163-8.
77. Voci, P., et al., *Coronary recanalization in anterior myocardial infarction: the open perforator hypothesis.* J Am Coll Cardiol, 2002. **40**(7): p. 1205-13.
78. Galderisi, M., et al., *Positive association between circulating free insulin-like growth factor-1 levels and coronary flow reserve in arterial systemic hypertension.* Am J Hypertens, 2002. **15**(9): p. 766-72.
79. Kondo, I., et al., *Ultrasonographic assessment of coronary flow reserve and abdominal fat in obesity.* Ultrasound Med Biol, 2001. **27**(9): p. 1199-205.
80. Galderisi, M., et al., *Coronary flow reserve and myocardial diastolic dysfunction in arterial hypertension.* Am J Cardiol, 2002. **90**(8): p. 860-4.
81. Bartel, T., et al., *Noninvasive assessment of microvascular function in arterial hypertension by transthoracic Doppler harmonic echocardiography.* J Am Coll Cardiol, 2002. **39**(12): p. 2012-8.

82. Vanderheyden, M., et al., *Non-invasive assessment of coronary flow reserve in idiopathic dilated cardiomyopathy: hemodynamic correlations.* Eur J Echocardiogr, 2005. **6**(1): p. 47-53.
83. Hildick-Smith, D.J., et al., *Coronary flow reserve is supranormal in endurance athletes: an adenosine transthoracic echocardiographic study.* Heart, 2000. **84**(4): p. 383-9.
84. Otsuka, R., et al., *Acute effects of passive smoking on the coronary circulation in healthy young adults.* JAMA, 2001. **286**(4): p. 436-41.
85. Kiviniemi, T.O., et al., *A moderate dose of red wine, but not de-alcoholized red wine increases coronary flow reserve.* Atherosclerosis, 2007. **195**(2): p. e176-81.
86. Voci, P., F. Pizzuto, and F. Romeo, *Coronary flow: a new asset for the echo lab?* Eur Heart J, 2004. **25**(21): p. 1867-79.
87. Sudhir, K., et al., *Assessment of coronary conductance and resistance vessel reactivity in response to nitroglycerin, ergonovine and adenosine: in vivo studies with simultaneous intravascular two-dimensional and Doppler ultrasound.* J Am Coll Cardiol, 1993. **21**(5): p. 1261-8.
88. Kiviniemi, T.O., et al., *Coronary artery diameter can be assessed reliably with transthoracic echocardiography.* Am J Physiol Heart Circ Physiol, 2004. **286**(4): p. H1515-20.
89. Kiviniemi, T.O., et al., *Vasodilation of epicardial coronary artery can be measured with transthoracic echocardiography.* Ultrasound Med Biol, 2007. **33**(3): p. 362-70.
90. Kaul, S., et al., *Incremental value of cardiac imaging in patients presenting to the emergency department with chest pain and without ST-segment elevation: a multicenter study.* Am Heart J, 2004. **148**(1): p. 129-36.
91. Jeetley, P., et al., *Myocardial contrast echocardiography for the detection of coronary artery stenosis: a prospective multicenter study in comparison with single-photon emission computed tomography.* J Am Coll Cardiol, 2006. **47**(1): p. 141-5.
92. Senior, R., et al., *Myocardial perfusion assessment in patients with medium probability of coronary artery disease and no prior myocardial infarction: comparison of myocardial contrast echocardiography with 99mTc single-photon emission computed tomography.* Am Heart J, 2004. **147**(6): p. 1100-5.
93. Picano, E., et al., *Stress echocardiography and the human factor: the importance of being expert.* J Am Coll Cardiol, 1991. **17**(3): p. 666-9.
94. Hoffmann, R., et al., *Analysis of interinstitutional observer agreement in interpretation of dobutamine stress echocardiograms.* J Am Coll Cardiol, 1996. **27**(2): p. 330-6.
95. Fleischmann, K.E., et al., *Exercise echocardiography or exercise SPECT imaging? A meta-analysis of diagnostic test performance.* JAMA, 1998. **280**(10): p. 913-20.
96. Derumeaux, G., et al., *Doppler tissue imaging quantitates regional wall motion during myocardial ischemia and reperfusion.* Circulation, 1998. **97**(19): p. 1970-7.
97. Vinereanu, D., A. Khokhar, and A.G. Fraser, *Reproducibility of pulsed wave tissue Doppler echocardiography.* J Am Soc Echocardiogr, 1999. **12**(6): p. 492-9.
98. Fraser, A.G., et al., *Feasibility and reproducibility of off-line tissue Doppler measurement of regional myocardial function during dobutamine stress echocardiography.* Eur J Echocardiogr, 2003. **4**(1): p. 43-53.
99. Schnackenburg, B., *Physical principles of MR imaging*, in *Cardiovascular Magnetic Resonance*, E. Nagel, A. van Rossum, and E. Fleck, Editors. 2004, Steinkopff Verlag: Darmstadt.
100. Grothues, F., et al., *Comparison of interstudy reproducibility of cardiovascular magnetic resonance with two-dimensional echocardiography in normal subjects and in patients with heart failure or left ventricular hypertrophy.* Am J Cardiol, 2002. **90**(1): p. 29-34.
101. Kim, R.J., et al., *Myocardial Gd-DTPA kinetics determine MRI contrast enhancement and reflect the extent and severity of myocardial injury after acute reperfused infarction.* Circulation, 1996. **94**(12): p. 3318-26.
102. Kim, R.J., et al., *Relationship of MRI delayed contrast enhancement to irreversible injury, infarct age, and contractile function.* Circulation, 1999. **100**(19): p. 1992-2002.

103. Mahrholdt, H., et al., *Reproducibility of chronic infarct size measurement by contrast-enhanced magnetic resonance imaging.* Circulation, 2002. **106**(18): p. 2322-7.
104. Ramani, K., et al., *Contrast magnetic resonance imaging in the assessment of myocardial viability in patients with stable coronary artery disease and left ventricular dysfunction.* Circulation, 1998. **98**(24): p. 2687-94.
105. Klein, C., et al., *Assessment of myocardial viability with contrast-enhanced magnetic resonance imaging: comparison with positron emission tomography.* Circulation, 2002. **105**(2): p. 162-7.
106. Kim, R.J., et al., *The use of contrast-enhanced magnetic resonance imaging to identify reversible myocardial dysfunction.* N Engl J Med, 2000. **343**(20): p. 1445-53.
107. Wellnhofer, E., et al., *Magnetic resonance low-dose dobutamine test is superior to SCAR quantification for the prediction of functional recovery.* Circulation, 2004. **109**(18): p. 2172-4.
108. Sharir, T., et al., *Prognostic value of poststress left ventricular volume and ejection fraction by gated myocardial perfusion SPECT in women and men: gender-related differences in normal limits and outcomes.* J Nucl Cardiol, 2006. **13**(4): p. 495-506.
109. Berman, D.S. and G. Germano, *The clinical value of assessing left ventricular function from gated SPECT perfusion studies.* Rev Port Cardiol, 2000. **19 Suppl 1**: p. I31-7.
110. Sharir, T., et al., *Incremental prognostic value of post-stress left ventricular ejection fraction and volume by gated myocardial perfusion single photon emission computed tomography.* Circulation, 1999. **100**(10): p. 1035-42.
111. Gibbons, R.J., et al., *The quantification of infarct size.* J Am Coll Cardiol, 2004. **44**(8): p. 1533-42.
112. O'Connor, M.K., et al., *Quantitative myocardial SPECT for infarct sizing: feasibility of a multicenter trial evaluated using a cardiac phantom.* J Nucl Med, 1995. **36**(6): p. 1130-6.
113. Fieno, D.S., et al., *Quantitation of infarct size in patients with chronic coronary artery disease using rest-redistribution Tl-201 myocardial perfusion SPECT: correlation with contrast-enhanced cardiac magnetic resonance.* J Nucl Cardiol, 2007. **14**(1): p. 59-67.
114. Klocke, F.J., et al., *ACC/AHA/ASNC guidelines for the clinical use of cardiac radionuclide imaging--executive summary: a report of the American College of Cardiology/American Heart Association Task Force on Practice Guidelines (ACC/AHA/ASNC Committee to Revise the 1995 Guidelines for the Clinical Use of Cardiac Radionuclide Imaging).* J Am Coll Cardiol, 2003. **42**(7): p. 1318-33.
115. Hendel, R.C., et al., *American Society of Nuclear Cardiology consensus statement: Reporting of radionuclide myocardial perfusion imaging studies.* J Nucl Cardiol, 2006. **13**(6): p. e152-6.
116. *Invasive compared with non-invasive treatment in unstable coronary-artery disease: FRISC II prospective randomised multicentre study. FRagmin and Fast Revascularisation during InStability in Coronary artery disease Investigators.* Lancet, 1999. **354**(9180): p. 708-15.
117. Schiller, N.B., et al., *Recommendations for quantitation of the left ventricle by two-dimensional echocardiography. American Society of Echocardiography Committee on Standards, Subcommittee on Quantitation of Two-Dimensional Echocardiograms.* J Am Soc Echocardiogr, 1989. **2**(5): p. 358-67.
118. Lang, R.M., et al., *Recommendations for chamber quantification.* Eur J Echocardiogr, 2006. **7**(2): p. 79-108.
119. Cerqueira, M.D., et al., *Standardized myocardial segmentation and nomenclature for tomographic imaging of the heart: a statement for healthcare professionals from the Cardiac Imaging Committee of the Council on Clinical Cardiology of the American Heart Association.* Circulation, 2002. **105**(4): p. 539-42.
120. Dahlberg, G., *Statistical methods for medical and biological students*. 2nd ed. 1940, London: George Allen&Unwin Ltd.
121. Lee, J., D. Koh, and C.N. Ong, *Statistical evaluation of agreement between two methods for measuring a quantitative variable.* Comput Biol Med, 1989. **19**(1): p. 61-70.

122. Rousson, V., T. Gasser, and B. Seifert, *Assessing intrarater, interrater and test-retest reliability of continuous measurements.* Stat Med, 2002. **21**(22): p. 3431-46.
123. Oppo, K., et al., *Doppler perfusion index: an interobserver and intraobserver reproducibility study.* Radiology, 1998. **208**(2): p. 453-7.
124. Peace, R.A., P.C. Adams, and J.J. Lloyd, *Effect of sex, age, and weight on ejection fraction and end-systolic volume reference limits in gated myocardial perfusion SPECT.* J Nucl Cardiol, 2008. **15**(1): p. 86-93.
125. Miller, T.D., et al., *Infarct size after acute myocardial infarction measured by quantitative tomographic 99mTc sestamibi imaging predicts subsequent mortality.* Circulation, 1995. **92**(3): p. 334-41.
126. Rosner, A., et al., *Left ventricular size determines tissue Doppler-derived longitudinal strain and strain rate.* Eur J Echocardiogr, 2008.
127. Baltabaeva, A., et al., *Regional left ventricular deformation and geometry analysis provides insights in myocardial remodelling in mild to moderate hypertension.* Eur J Echocardiogr, 2008. **9**(4): p. 501-8.
128. Kuvin, J.T., et al., *Peripheral vascular endothelial function testing as a noninvasive indicator of coronary artery disease.* J Am Coll Cardiol, 2001. **38**(7): p. 1843-9.
129. Daimon, M., et al., *Physiologic assessment of coronary artery stenosis by coronary flow reserve measurements with transthoracic Doppler echocardiography: comparison with exercise thallium-201 single piston emission computed tomography.* J Am Coll Cardiol, 2001. **37**(5): p. 1310-5.
130. Fujimoto, K., et al., *New noninvasive diagnosis of myocardial ischemia of the left circumflex coronary artery using coronary flow reserve measurement by transthoracic Doppler echocardiography: comparison with thallium-201 single photon emission computed tomography.* J Cardiol, 2004. **43**(3): p. 109-16.
131. Hirata, K., et al., *Noninvasive diagnosis of restenosis by transthoracic Doppler echocardiography after percutaneous coronary intervention: comparison with exercise Tl-SPECT.* J Am Soc Echocardiogr, 2006. **19**(2): p. 165-71.
132. Rigo, F., et al., *Transthoracic echocardiographic imaging of coronary arteries: tips, traps, and pitfalls.* Cardiovasc Ultrasound, 2008. **6**: p. 7.
133. Winter, R., P. Gudmundsson, and R. Willenheimer, *Feasibility of noninvasive transthoracic echocardiography/Doppler measurement of coronary flow reserve in left anterior descending coronary artery in patients with acute coronary syndrome: a new technique tested in clinical practice.* J Am Soc Echocardiogr, 2003. **16**(5): p. 464-8.
134. Voci, P., et al., *Measurement of coronary flow reserve in the anterior and posterior descending coronary arteries by transthoracic Doppler ultrasound.* Am J Cardiol, 2002. **90**(9): p. 988-91.
135. Peteiro, J., et al., *Comparison of two-dimensional echocardiography and pulsed Doppler tissue imaging during dobutamine-atropine stress testing to detect coronary artery disease.* Echocardiography, 2001. **18**(4): p. 275-84.
136. Madler, C.F., et al., *Non-invasive diagnosis of coronary artery disease by quantitative stress echocardiography: optimal diagnostic models using off-line tissue Doppler in the MYDISE study.* Eur Heart J, 2003. **24**(17): p. 1584-94.
137. Heimdal, A., et al., *Real-time strain rate imaging of the left ventricle by ultrasound.* J Am Soc Echocardiogr, 1998. **11**(11): p. 1013-9.
138. Helle-Valle, T., et al., *New noninvasive method for assessment of left ventricular rotation: speckle tracking echocardiography.* Circulation, 2005. **112**(20): p. 3149-56.
139. Lyseggen, E., et al., *Myocardial strain analysis in acute coronary occlusion: a tool to assess myocardial viability and reperfusion.* Circulation, 2005. **112**(25): p. 3901-10.
140. Bjork Ingul, C., et al., *Incremental value of strain rate imaging to wall motion analysis for prediction of outcome in patients undergoing dobutamine stress echocardiography.* Circulation, 2007. **115**(10): p. 1252-9.

141. Dickstein, K., et al., *ESC Guidelines for the diagnosis and treatment of acute and chronic heart failure 2008 The Task Force for the Diagnosis and Treatment of Acute and Chronic Heart Failure 2008 of the European Society of Cardiology. Developed in collaboration with the Heart Failure Association of the ESC (HFA) and endorsed by the European Society of Intensive Care Medicine (ESICM).* Eur J Heart Fail, 2008.
142. Hohnloser, S.H., et al., *Prevalence, characteristics and prognostic value during long-term follow-up of nonsustained ventricular tachycardia after myocardial infarction in the thrombolytic era.* J Am Coll Cardiol, 1999. **33**(7): p. 1895-902.
143. Routledge, H.C., D.W. Rea, and R.P. Steeds, *Monitoring the introduction of new drugs--Herceptin to cardiotoxicity.* Clin Med, 2006. **6**(5): p. 478-81.
144. Gudmundsson, P., et al., *Visually estimated left ventricular ejection fraction by echocardiography is closely correlated with formal quantitative methods.* Int J Cardiol, 2005. **101**(2): p. 209-12.
145. van Royen, N., et al., *Comparison and reproducibility of visual echocardiographic and quantitative radionuclide left ventricular ejection fractions.* Am J Cardiol, 1996. **77**(10): p. 843-50.
146. McGowan, J.H. and J.G. Cleland, *Reliability of reporting left ventricular systolic function by echocardiography: a systematic review of 3 methods.* Am Heart J, 2003. **146**(3): p. 388-97.
147. Corsi, C., et al., *Left ventricular volume estimation for real-time three-dimensional echocardiography.* IEEE Trans Med Imaging, 2002. **21**(9): p. 1202-8.
148. Jurcut, R., et al., *Detection of regional myocardial dysfunction in patients with acute myocardial infarction using velocity vector imaging.* J Am Soc Echocardiogr, 2008. **21**(8): p. 879-86.